

## LEADING AND NEXT-TO-LEADING QCD CORRECTIONS TO $\varepsilon$ -PARAMETER AND $B^0$ – $\bar{B}^0$ MIXING IN THE PRESENCE OF A HEAVY TOP QUARK

Andrzej J. BURAS<sup>1,2</sup>, Matthias JAMIN<sup>1</sup> and Peter H. WEISZ<sup>2</sup>

<sup>1</sup>Physik Department, Technische Universität München, D-8046 Garching, FRG

<sup>2</sup>Max-Planck-Institut für Physik und Astrophysik–Werner-Heisenberg-Institut für Physik,  
P.O. Box 40 12 12, D-8000 München, FRG

Received 22 March 1990

We present a complete calculation of leading and next-to-leading QCD corrections to the QCD factors  $\eta_{2K}$  and  $\bar{\eta}_{2B}$ , relevant for the  $CP$ -violating  $\varepsilon$ -parameter and  $B^0$ – $\bar{B}^0$  mixing in the presence of a heavy top quark. We demonstrate explicitly that the resulting  $\eta_2$ 's are gauge as well as renormalization prescription independent. We also show that they do not depend on the infrared structure of the theory. We emphasize that these results only follow after correct factorization of short and long distance contributions, which has not been done properly in many recent QCD analyses present in the literature. We stress however that  $\eta_2(x_1)$  with  $x_1 = m_t^2/M_W^2$  depends sensitively on the definition of the top quark mass and only the product  $\eta_2(x_1)S(x_1)$  ( $S(x_1)$  being the function resulting from the lowest order box diagram) is free from this dependence. For  $m_t = \bar{m}_t(M_W)$  the corresponding  $\eta_2$ 's decrease strongly with  $m_t$ , whereas for  $m_t^* = \bar{m}_t(m_t)$  they show only a weak  $m_t^*$ -dependence:  $0.58 \geq \eta_{2K}^* \geq 0.56$  and  $0.88 \geq \bar{\eta}_{2B}^* \geq 0.84$  for  $60 \text{ GeV} \leq m_t^* \leq 300 \text{ GeV}$  and  $\Lambda_{\overline{MS}} = 200 \text{ MeV}$ . A critical discussion of the existing literature on QCD calculations in the presence of a large  $m_t$  is presented.

### 1. Introduction

The flavour-changing neutral current processes (FCNC) such as the particle–antiparticle mixing, certain rare meson decays and  $CP$ -violating decays have played an important role in particle physics over the last two decades. In addition to constraining the physics beyond the Standard Model, they served in bounding the parameters of the Standard Model, such as the elements of the Cabibbo–Kobayashi–Maskawa (CKM) matrix [1] and the masses of the quarks. The prime example is the  $K^0$ – $\bar{K}^0$  mixing which, in the sixties and early seventies, led not only to the conjecture of the existence of the charm quark [2], but also allowed a successful estimate of its mass prior to its discovery [3]. In the case of the top quark these days a similar role is played by  $B^0$ – $\bar{B}^0$  mixing and  $CP$  violation in  $K \rightarrow \pi\pi$  decays, which also serve to constrain the  $CP$ -violating phase  $\delta$  in the CKM matrix.

Although the FCNC processes originate through weak interactions, they are influenced by QCD effects at both long and short distances. Whereas the long distance QCD effects must be evaluated by means of nonperturbative techniques (albeit a very difficult task), the short distance QCD effects can be systematically evaluated due to asymptotic freedom in the framework of renormalization group improved perturbation theory. They are contained in the Wilson coefficient functions of the relevant local operators built out of quark and gluon fields.

Until recently most of the calculations of weak decays present in the literature [4–8] included only QCD effects in the leading logarithmic approximation and assumed that  $m_t \ll M_W$ . These include in particular the calculations by Gilman and Wise [5, 8] which have been utilized by many researchers in the field. In view of the rapidly increasing lower bound on  $m_t$ , the analysis of Gilman and Wise has to be modified in order to properly take heavy top quark effects into account. During the last year a number of papers [9–14] appeared which generalized at least approximately the usual renormalization group analysis to include heavy top quark effects in various FCNC processes.

The basic idea of refs. [9–14] is very simple. One calculates the one-loop contributions (box diagram and penguin diagrams) to a given process with the full W-boson and top quark propagators taken into account exactly, i.e. to all orders in  $m_t^2/M_W^2$ . The result of this calculation then serves as the initial condition at  $\mu = M_W$  to the renormalization group equations for the Wilson coefficient functions of the relevant operators. The renormalization group transformation to low energy scales is performed consecutively in the effective five-\*, four- and three-quark theory in the leading logarithmic approximation in the same manner as in the original analysis of Gilman and Wise. More involved considerations of heavy quark effects which attempt to go beyond the treatment of refs. [9–14], have been presented in refs. [15–18]. These papers deal only with particle–antiparticle mixing. We will discuss them in sect. 6.

Although the treatment of refs. [9–14] may at the end turn out to be a reasonable approximation to a complete analysis, it is for several reasons not fully satisfactory. In order to see this clearly let us consider the effective hamiltonian for  $\Delta S = 2$  transitions

$$H_{\text{eff}} = \frac{G_F^2}{16\pi^2} M_W^2 [\lambda_c^2 \eta_1 S(x_c) + \lambda_t^2 \eta_2 S(x_t) + 2\lambda_c \lambda_t \eta_3 S(x_c, x_t)] [\alpha_3(\mu)]^{-2/9} \hat{O}_{LL}(\mu), \quad (1.1)$$

where

$$\hat{O}_{LL} = (\bar{s} \gamma_\mu (1 - \gamma_5) d) (\bar{s} \gamma^\mu (1 - \gamma_5) d) \equiv (\bar{s} d)_{V-A} (\bar{s} d)_{V-A}, \quad (1.2)$$

\* The top quark has been integrated out in the first step of the analysis.

$x_i = m_i^2/M_W^2$  and  $\lambda_i = V_{id}V_{is}^*$ , with  $V_{ij}$  being the elements of the CKM matrix.  $S(x_i)$  and  $S(x_i, x_j)$  are the Inami–Lim functions [19], which are obtained by evaluating the usual box diagrams for arbitrary values of the internal quark masses. An explicit expression for  $S(x_i)$  is given in eq. (2.4). The parameters  $\eta_i$  represent QCD corrections to the box diagrams. In the absence of QCD corrections  $\eta_i = 1$ . The parameters  $\eta_1$  and  $\eta_3$  are complicated functions of

$$\alpha_f(Q) = \frac{12\pi}{(33-2f)\ln Q^2/\Lambda_f^2}, \quad f=3,4,5, \quad (1.3)$$

the running QCD coupling constant  $\alpha_f$  relevant for an effective theory with  $f$  quark flavours,  $\Lambda_f$  denoting the corresponding QCD scale parameters.

In the case of a heavy top quark a much simpler expression can be found for  $\eta_2$ . Setting  $m_t = M_W^*$  in the formula of Gilman and Wise [8], one finds immediately [13, 14]

$$\eta_2 = [\alpha_3(m_c)]^{6/27} \left[ \frac{\alpha_4(m_b)}{\alpha_4(m_c)} \right]^{6/25} \left[ \frac{\alpha_5(M_W)}{\alpha_5(m_b)} \right]^{6/23}. \quad (1.4)$$

In writing eq. (1.1) we have factored out the  $\mu$ -dependence usually present in  $\eta_2$ , so that

$$B_K = B_K(\mu) [\alpha_3(\mu)]^{-2/9}, \quad (1.5)$$

with

$$\langle \bar{K}^0 | \hat{O}_{LL}(\mu) | K^0 \rangle \equiv \frac{8}{3} B_K(\mu) F_K^2 m_K^2, \quad (1.6)$$

is renormalization group invariant. In the spirit of the method of refs. [9–14],  $S(x_i)$  plays the role of the initial condition (taken at  $M_W$ ) to the renormalization group equation for the Wilson coefficient function of the operator  $\hat{O}_{LL}$ . The renormalization group transformation to low energy scales is then represented by  $\eta_2$ . Although all this looks very reasonable, two immediate questions arise:

- (i) Why should the initial condition for the Wilson coefficient function of  $\hat{O}_{LL}$  be equal to the value obtained in the free field theory?
- (ii) Why should the initial condition be taken at  $M_W$  rather than at  $\sqrt{2}M_W$ ,  $2M_W$  or any other scale  $O(M_W)$ ?

The usual argument in refs. [9–14], put forward in favour of (i), is that at a high scale such as  $M_W$ , the QCD corrections are so small that they can be neglected. Yet without any explicit calculation it is difficult to justify this assumption. Similar

\* In the leading logarithmic approximation there is no distinction between  $m_t$  and  $M_W$  as long as  $m_t = O(M_W)$  and no large  $\ln x_i$  are present. The choice  $m_t = M_W$  is then the simplest one. See subsect. 5.6 for a discussion of the scales in the leading term.

arguments are used in connection with (ii). If the QCD coupling is small at  $M_W$ , the running of  $\alpha$  in the neighbourhood of  $M_W$  is also small, and consequently it should not matter whether the free field theory is assumed at  $M_W, \sqrt{2}M_W, 2M_W$  etc. Yet as one can easily verify by using eq. (1.4), the final result depends on the particular choice. This feature of eq. (1.4) breaks the basic principle of renormalization group invariance, which states, that the final result for the Wilson coefficient functions must not depend on the scale at which the boundary conditions are assumed. There are two other evident questions:

- (iii) Restricting our attention to the second term of eq. (1.1), how should the top quark mass be defined? Should it be  $\bar{m}_t(M_W)$ ,  $\bar{m}_t(2M_W)$ ,  $\bar{m}_t(m_t)$  or anything else?
- (iv) What value of  $A_f$  should be used in eqs. (1.3) and (1.4)? Although  $\alpha_s(M_W)$  is not particularly sensitive to this value, this is no longer the case for  $\alpha_s(m_c)$ .

In particular question (iii) is of phenomenological importance, because  $S(x_t)$  is a sensitive function of  $m_t$ . One can convince oneself by using eq. (2.4) that for a very heavy top quark the choices  $\bar{m}_t(M_W)$  and  $\bar{m}_t(m_t)$  give results for  $S(x_t)$  differing by as much as 20%, which obviously is rather disturbing.

As we will demonstrate in this paper all four questions can be answered, once the next-to-leading order corrections to  $H_{\text{eff}}$  of eq. (1.1) have been taken into account. We will see that:

- (i') the initial conditions for the Wilson coefficient functions indeed differ from the free field theory values,
- (ii') the final result for  $\eta_2$  does not depend on the scale at which the initial conditions have been imposed,
- (iii') although both  $\eta_2$  and  $S(x_t)$  depend on the definition of  $m_t$ , the product  $\eta_2(x_t)S(x_t)$  and the resulting physical predictions are independent of a given choice as they should, and
- (iv') the presence of next-to-leading order corrections calculated in the  $\overline{\text{MS}}$  scheme will allow us to replace  $A_f$  in eq. (1.3) by  $(A_f)_{\overline{\text{MS}}}$ , extracted say from the data on deep-inelastic scattering.

As we already stated above, it turns out that the analysis is very involved in the case of  $\eta_1$  and  $\eta_3$ . Therefore in the present paper we will concentrate on  $\eta_2$  for which the calculation, although tedious, is considerably simpler. Moreover it is precisely  $\eta_2$  which is of main interest to us. Indeed the second term in eq. (1.1) gives the dominant contribution to the  $CP$ -violating  $\varepsilon$ -parameter in  $K \rightarrow \pi\pi$  decays and to  $B^0-\bar{B}^0$  mixing (for  $\Delta B = 2$ ) which, as stated above, plays important roles in present day phenomenology.

At this stage it should be mentioned that steps towards the inclusion of next-to-leading QCD corrections into the effective hamiltonian of eq. (1.1) have already been made in refs. [15,17]. In our opinion these attempts are basically incorrect (see sect. 6).

A consistent procedure for the calculation of the next-to-leading terms in the renormalization group improved perturbation theory for the Wilson coefficient

functions of local operators has been laid out as early as in 1978 in the papers of Bardeen et al. [20] and Floratos et al. [21]. In these papers this procedure has been used to calculate for the first time the next-to-leading QCD corrections to a short distance process: deep inelastic e-p scattering. This method, consisting of three distinct but interrelated steps, is completely general and can also be applied to weak decays. The only new important feature of the application presented here is the one related to the definition of  $m_t$  which, however, can be incorporated without any difficulty. Recently we used the procedure of refs. [20,21] to calculate next-to-leading QCD corrections to the  $\Delta S = 1$  hamiltonian [22]. Since the result of this calculation will be needed in the course of our analysis, we will comment on it in subsect. 4.1. Each of the three steps involved contains a number of subtleties which one has to properly deal with, in order to obtain the correct result.

Before presenting the three steps in detail, let us first state the main point of refs. [20,21] which is crucial for the evaluation of the next-to-leading QCD corrections to the Wilson coefficient functions of local operators. We recall that the Wilson coefficient functions depend only on the short distance structure of the theory and consequently (at the same time fortunately) do not depend on the long distance structure of QCD which is at present rather poorly calculable. In particular they do not depend on the properties of external states in a given process. Thus in principle for the case at hand, the Wilson coefficient function  $C_{LL}$  of the operator  $\hat{O}_{LL}$  is directly obtainable from the operator product expansion of the product of four weak currents, which is certainly only connected to the short distance structure of the theory. This direct procedure for finding  $C_{LL}$  is however rather cumbersome. It turns out that a more efficient method is to calculate some relevant process, from which a particular coefficient function can be extracted. Using the property that the Wilson coefficient functions do not depend on the states between which the operators are sandwiched, we can choose any process for which perturbative calculations can be performed. Consequently in the case at hand, we can study the amplitude

$$A(\bar{s}d \rightarrow \bar{d}s) \equiv \langle H_{\text{eff}} \rangle = C_{LL}(\mu) \langle \hat{O}_{LL}(\mu) \rangle, \quad (1.7)$$

where  $\langle \dots \rangle$  denotes the matrix element between the quark states and  $C_{LL}$  is the Wilson coefficient function in question. Evaluating  $A(\bar{s}d \rightarrow \bar{d}s)$  and  $\langle \hat{O}_{LL}(\mu) \rangle$  leads to  $C_{LL}(\mu)$ .

Restricting our attention to the effective hamiltonian of eq. (1.1), the three steps from which  $C_{LL}$  can be found are as follows:

*Step 1.* One first calculates the  $O(\alpha)$  corrections to the box diagram of fig. 1 in order to find  $\langle H_{\text{eff}} \rangle$  to  $O(\alpha)$ . The contributing diagrams are given in fig. 2. The result of this calculation depends in general on the gauge for the gluon propagator and on the particular assumptions about the external quarks. Now as stated above the Wilson coefficient functions cannot depend on the external states and must

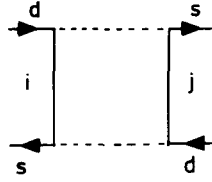


Fig. 1. The box diagram contributing to the effective hamiltonian for  $\Delta S = 2$  transitions in the absence of QCD corrections. The dashed lines stand for  $W^\pm$  and the corresponding fictitious Higgs exchanges.

also be gauge independent. In contrast to refs. [15,17] we therefore strongly emphasize that the result for the diagrams of fig. 2 *cannot* by itself be used to obtain the Wilson coefficient functions of local operators. The result for the diagrams of fig. 2 merely represents the product of the Wilson coefficient functions and the “matrix elements” of local operators between quark states as explicitly given in eq. (1.7). The gauge dependence which was found, as well as the dependence on the external states, are simply remnants of the matrix elements which contain long distance contributions. In the actual calculation one cannot set all masses and momenta of the external quarks to zero since this would result in

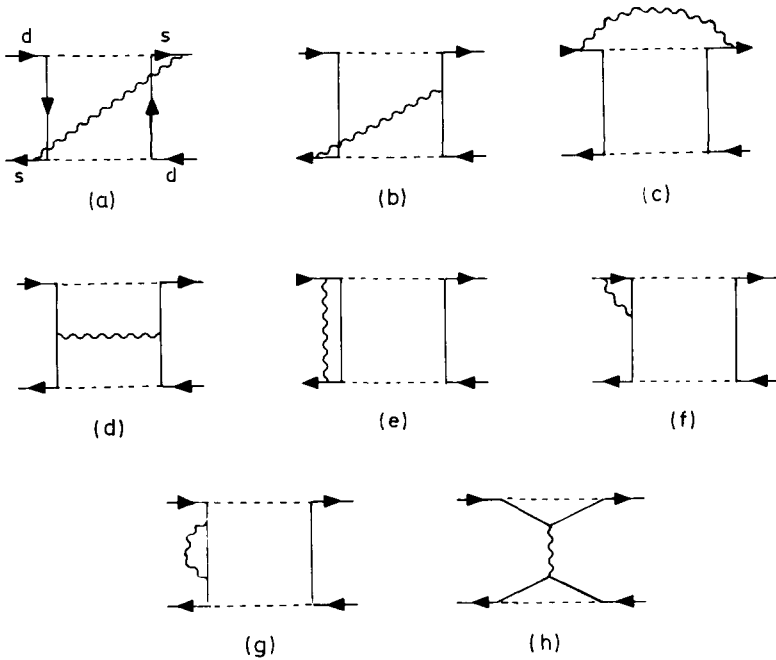


Fig. 2. QCD corrections to the box diagram of fig. 1. The remaining diagrams are obtained by interchanging the external lines.

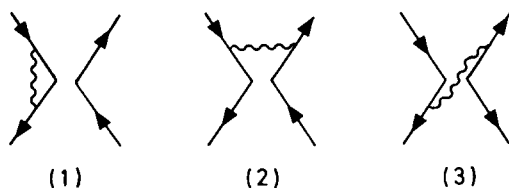


Fig. 3. QCD corrections to the matrix element of  $\hat{O}_{LL}$  between quark states.

infrared divergences. We performed two calculations in which we either kept the external quark masses or nonvanishing external momenta wherever this was necessary to prevent divergences. The results of these two calculations differ. In particular in both cases new operators that are not of the  $(V-A) \otimes (V-A)$  type appear.

*Step 2.* In order to proceed further, we have to perform factorization of short and long distance contributions to the diagrams of fig. 2. This is done by simply evaluating the matrix elements of local operators between quark states (see fig. 3), i.e.  $\langle \hat{O}_{LL}(\mu) \rangle$  of eq. (1.7). Comparing the result after renormalization with the result for  $\langle H_{\text{eff}} \rangle$ , one immediately finds the Wilson coefficient function  $C_{LL}(\mu)$ . It is however crucial that, whatever treatment is applied to the external quarks, it has to be the same for the diagrams of figs. 2 and 3. After the factorization has been done properly, the gauge dependence, the dependence on the infrared behaviour, as well as the presence of additional operators are attributed to  $\langle \hat{O}_{LL}(\mu) \rangle$ , leaving  $C_{LL}(\mu)$  free of gauge dependence and the dependence on the external states. The resulting Wilson coefficient function depends however on the ultraviolet renormalization of  $\hat{O}_{LL}$ . This dependence will be removed in the following step.

*Step 3.* The calculation of the Wilson coefficient functions is not yet complete, because at the next-to-leading level in the renormalization group improved perturbation theory, one also has to include additional contributions, in particular the two-loop anomalous dimension of  $\hat{O}_{LL}$ . The latter also depends on the renormalization scheme, and this dependence cancels the one found in Step 2 so that the final Wilson coefficient function of  $\hat{O}_{LL}$  is independent of the renormalization scheme as it should be. Explicit examples of this feature have been discussed in ref. [22]. Additional contributions also come from the two-loop  $\beta$ -function. They do however not depend on the renormalization scheme. It is this step in which one has to deal with the questions (i) to (iv) posed above.

The following three sections constitute an explicit realization of the procedure outlined above, as applied to the calculation of  $\eta_2$ . In short, sects. 2–4 are devoted to steps 1–3 respectively. The main results of our paper are stated and evaluated numerically in sect. 5. These are the values for  $\eta_2$ , relevant for the parameter  $\varepsilon$  and  $B^0-\bar{B}^0$  mixing, with leading and next-to-leading QCD corrections fully taken into account.

In sect. 6, we compare our results with those obtained by Yao and collaborators [15–17], and also discuss the paper of Datta et al. [18]. Sect. 7 contains a summary of our paper.

An important aspect of our paper is the analysis of the dependence of  $\eta_2$  on the definition of the top quark mass. This dependence can only be meaningfully studied, and removed from the effective hamiltonian, by properly including the next-to-leading QCD corrections. In fact, only the product  $\eta_2(x_t)S(x_t)$  is free from this dependence, as formally expressed in eq. (5.1). To our knowledge, this feature has so far not been discussed in the literature. It is certainly an important ingredient in QCD calculations for FCNC processes in which the  $m_t$ -dependence already appears in the leading term.

We find that for  $m_t = \bar{m}_t(M_W)$  the corresponding  $\eta_2$ 's decrease strongly with  $m_t$ , so that e.g. for  $m_t = 300$  GeV,  $\eta_{2K} = 0.47$ , to be compared with  $(\eta_{2K})_{LO} = 0.62$  obtained in the leading order. On the other hand, for  $m_t^* = \bar{m}_t(m_t)$  the corresponding  $\eta_2^*$ 's show only a weak  $m_t^*$ -dependence and do not differ considerably from the values for  $\eta_2$  used in the literature. For  $A_{\overline{MS}} = 200$  MeV and  $60 \text{ GeV} \leq m_t^* \leq 300 \text{ GeV}$  we find  $0.58 \geq \eta_{2K}^* \geq 0.56$  and  $0.88 \geq \bar{\eta}_{2B}^* \geq 0.84$ . In any case, we conclude that even for  $m_t \approx 300$  GeV the QCD renormalization group improved perturbation theory works quite well. For still higher values of  $m_t$ , one has in any case to worry about the perturbation theory in the weak coupling due to the very large top–Higgs Yukawa couplings. We will comment on this at the end of our paper.

## 2. Explicit QCD corrections to the box diagram

### 2.1. FREE QUARK RESULT

In the absence of QCD corrections, the effective hamiltonian for  $\Delta S = 2$  transitions is obtained from the diagram of fig. 1. Neglecting external momenta and masses one finds

$$\langle H_{\text{eff}} \rangle^{(0)} = \frac{G_F^2}{16\pi^2} M_W^2 \sum_{i,j} \lambda_i \lambda_j \tilde{S}(x_i, x_j) \langle \hat{O}_{LL} \rangle^{(0)}, \quad (2.1)$$

where  $x_i = m_i^2/M_W^2$  with  $i = u, c, t$ , the operator  $\hat{O}_{LL}$  is given in eq. (1.2), and

$$\tilde{S}(x_i, x_j) = \left(1 + \frac{1}{4}x_i x_j\right) A(x_i, x_j) - 2x_i x_j B(x_i, x_j). \quad (2.2)$$

The functions  $A(x_i, x_j)$  and  $B(x_i, x_j)$  are given in appendix A. We note a characteristic structure in eq. (2.2) which we will also encounter in some diagrams of fig. 2. The first two terms result from WW and HH exchanges, whereas the last term arises from WH and HW exchanges. Similar to eq. (1.7)  $\langle \hat{O}_{LL} \rangle^{(0)}$  denotes the leading order matrix element of  $\hat{O}_{LL}$  between external quark states.



In order to cast eq. (2.1) into the form analogous to (1.1), one uses the unitarity of the CKM matrix, i.e.  $\sum_i \lambda_i = 0$ . This gives eq. (1.1) with  $\eta_i = 1$ , and e.g.

$$S(x_t) = \tilde{S}(x_t, x_t) - 2\tilde{S}(x_t, x_u) + \tilde{S}(x_u, x_u). \quad (2.3)$$

For  $x_u = 0$  one then finds the familiar expression

$$S(x_t) = x_t \left[ \frac{1}{4} + \frac{9}{4} \frac{1}{(1-x_t)} - \frac{3}{2} \frac{1}{(1-x_t)^2} \right] - \frac{3}{2} \left[ \frac{x_t}{1-x_t} \right]^3 \ln x_t. \quad (2.4)$$

## 2.2. GENERAL STRUCTURE OF $O(\alpha_{\text{QCD}})$ CORRECTIONS

The  $O(\alpha_{\text{QCD}})$  corrections to the  $\Delta S = 2$  transition are represented by the diagrams of fig. 2. Let us denote by  $\hat{1}$  and  $t^a = \lambda^a/2$  ( $a = 1, \dots, N^2 - 1$ ) the  $N \times N$  matrices in colour space, with  $\lambda^a$  being the Gell-Mann matrices and  $N$  denoting the number of colours. Because the diagrams in fig. 2 contain two separate quark lines, the colour factors have the structure of tensor products in colour space. The diagrams (a)–(d) have the “octet” structure  $t^a \otimes t^a$ , whereas the diagrams (e)–(g) have the “singlet” structure  $\hat{1} \otimes \hat{1}$ .

The diagrams (f) and (g) are ultraviolet divergent and have to be renormalized. We have performed the renormalization in the  $\overline{\text{MS}}$  scheme. It should be stressed that in view of the presence of Higgs quark couplings which are proportional to quark masses, both the wave function renormalization and the mass renormalization have to be performed in the case of the diagram (f). In the actual calculation we used the dimensional regularization scheme (DR) with anticommuting  $\gamma_5$ . In view of our previous work [22], this method is justified in the case considered.

As already mentioned, the diagrams (a), (c) and (e) would contain infrared divergences if we were to set all external masses and momenta to zero. The simplest way to circumvent these divergences is to keep the external quark masses whenever necessary, but set them to zero otherwise. This is what we will do first. Another way would be to keep nonvanishing external momenta and setting all quark masses to zero. We have performed this second treatment as well and will comment on it in the next section.

Finally the diagrams (b) and (d) are both ultraviolet and infrared finite. We have not included the diagram (h) since it vanishes in the limit of zero external momenta.

The correction to the matrix element of the effective hamiltonian of eq. (2.1) between external quark states, resulting from the diagrams of fig. 2, is given as follows

$$\langle \Delta H_{\text{eff}} \rangle = \frac{G_F^2}{16\pi^2} M_W^2 \frac{\alpha}{4\pi} \sum_{i,j} \lambda_i \lambda_j U(x_i, x_j), \quad (2.5)$$

where

$$U(x_i, x_j) = \sum_k \left\langle \left[ C_F \hat{1} \otimes \hat{1} V_k^{(1)}(x_i, x_j) + t^a \otimes t^a V_k^{(8)}(x_i, x_j) \right] \hat{T}_k \right\rangle, \quad (2.6)$$

with  $k = \text{LL}, 1, 2, 3$ , and  $C_F = (N^2 - 1)/2N$ . The spinor structures  $\hat{T}_k$  are given by

$$\hat{T}_{\text{LL}} = \gamma_\mu L \otimes \gamma^\mu L, \quad \hat{T}_1 = L \otimes L - \frac{1}{4} \sigma_{\mu\nu} L \otimes \sigma^{\mu\nu} L + (L \rightarrow R), \quad (2.7)$$

$$\hat{T}_2 = L \otimes R + R \otimes L, \quad \hat{T}_3 = \gamma_\mu L \otimes \gamma^\mu R + \gamma_\mu R \otimes \gamma^\mu L, \quad (2.8)$$

with  $L = (1 - \gamma_5)$  and  $R = (1 + \gamma_5)$ . The additional tensors  $\hat{T}_1$ ,  $\hat{T}_2$  and  $\hat{T}_3$  originate from the diagrams (a), (c) and (e) respectively. In writing eqs. (2.7) and (2.8) we have only shown the tensor structure of these objects. The products of tensor products in Dirac and colour space should be understood as follows

$$\hat{1} \otimes \hat{1} \hat{T}_{\text{LL}} = (\bar{s}_i \gamma_\mu (1 - \gamma_5) d_i) (\bar{s}_j \gamma^\mu (1 - \gamma_5) d_j) = \hat{O}_{\text{LL}}, \quad (2.9)$$

$$t^a \otimes t^a \hat{T}_{\text{LL}} = (\bar{s}_i \gamma_\mu (1 - \gamma_5) t_{ij}^a d_j) (\bar{s}_k \gamma^\mu (1 - \gamma_5) t_{kl}^a d_l), \quad (2.10)$$

and similarly for the other tensors.

In view of the fact that  $\hat{O}_{\text{LL}}$  is self-conjugate under the Fierz transformation, one can in this case make the following replacement

$$t^a \otimes t^a \rightarrow \frac{1}{2} \left( 1 - \frac{1}{N} \right) \hat{1} \otimes \hat{1}. \quad (2.11)$$

However it will be useful to keep for some time the distinction between octet and singlet contributions.

In order to have a better control over the calculation, we have worked in an arbitrary covariant  $\xi$ -gauge for the gluon propagator. The  $W$ -propagators have been taken in the 't Hooft–Feynman gauge. The results for the coefficients  $V_k^{(1)}(x_i, x_j)$  and  $V_k^{(8)}(x_i, x_j)$  are

$$\begin{aligned} V_{\text{LL}}^{(8)}(x_i, x_j) &= L^{(8)}(x_i, x_j) + 2\xi \tilde{S}(x_i, x_j) + (3 + \xi) \ln x_d x_s \tilde{S}(x_i, x_j) \\ &\quad - 2\xi \frac{1}{x_d - x_s} [x_d \ln x_d - x_s \ln x_s] \tilde{S}(x_i, x_j), \end{aligned} \quad (2.12)$$

$$\begin{aligned} V_{\text{LL}}^{(1)}(x_i, x_j) &= L^{(1)}(x_i, x_j) + 2\xi \tilde{S}(x_i, x_j) - 2\xi \frac{1}{x_d - x_s} [x_d \ln x_d - x_s \ln x_s] \tilde{S}(x_i, x_j) \\ &\quad + 2\xi \ln x_\mu \tilde{S}(x_i, x_j) + 6 \ln x_\mu \left( x_i \frac{\partial}{\partial x_i} + x_j \frac{\partial}{\partial x_j} \right) \tilde{S}(x_i, x_j), \end{aligned} \quad (2.13)$$

$$V_1^{(8)}(x_i, x_j) = -(3 + \xi) \tilde{S}(x_i, x_j), \quad (2.14)$$

$$V_2^{(8)}(x_i, x_j) = -2V_3^{(1)}(x_i, x_j) = -(3 + \xi) \tilde{S}(x_i, x_j) \frac{m_d m_s}{m_d^2 - m_s^2} \ln \frac{x_d}{x_s}, \quad (2.15)$$

with the remaining coefficients being zero. Here  $x_\mu = \mu^2/M_W^2$ .

We would like to make the following comments:

(i) The terms  $L^{(8)}(x_i, x_j)$  and  $L^{(1)}(x_i, x_j)$  are complicated functions of  $x_i$  and  $x_j$ , which are collected in appendix B. They are both gauge independent. It should however be mentioned that the separate contributions to  $L^{(8)}(x_i, x_j)$  and  $L^{(1)}(x_i, x_j)$  are gauge dependent. Denoting the gauge dependent parts of a given diagram by  $G_k$ , we find the following relations

$$G_d = G_a + G_c, \quad G_b = -2G_d, \quad G_e = G_g = -\frac{1}{2}G_f \quad (2.16)$$

from which the gauge independence of the  $L^{(i)}$  follows.

(ii) Most of the remaining terms in eqs. (2.12)–(2.15) are gauge dependent and in addition exhibit the dependence on the external quarks. They are all proportional to  $\tilde{S}(x_i, x_j)$ , which, as we shall see in the next section, is crucial for the factorization of short and long distance contributions.

(iii) The  $\mu$ -dependence in eq. (2.13) is a consequence of the renormalization. We note that the last term in (2.13) is gauge independent. As we will see in subsect. 4.1, this term is responsible for the running of the internal quark masses.

We finish this section with a word of caution. The ultraviolet divergent diagrams (f) and (g) contain the box diagram of fig. 1 as a subdiagram. In spite of this fact, the  $O(\varepsilon)$  contributions to the box diagram have to be taken into account for the counterterms.

### 3. Wilson coefficient function of $\hat{O}_{LL}$ to $O(\alpha_{QCD})$

The matrix element of the effective hamiltonian to  $O(\alpha_{QCD})$  is given by

$$\langle H_{\text{eff}} \rangle = \langle H_{\text{eff}} \rangle^{(0)} + \langle \Delta H_{\text{eff}} \rangle, \quad (3.1)$$

with  $\langle H_{\text{eff}} \rangle^{(0)}$  and  $\langle \Delta H_{\text{eff}} \rangle$  given in eqs. (2.1) and (2.5) respectively. As is evident from eq. (2.6),  $\langle H_{\text{eff}} \rangle$  is a linear combination of the tensors  $\hat{T}_k$  ( $k = LL, 1, 2, 3$ ), with coefficients that are gauge dependent, and contain the dependence on the external quarks.

The purpose of this section is to demonstrate that  $\langle H_{\text{eff}} \rangle$  can be written in a factorized form

$$\langle H_{\text{eff}} \rangle = \frac{G_F^2}{16\pi^2} M_W^2 \sum_{i,j} \lambda_i \lambda_j \tilde{C}_{LL}(x_i, x_j, x_\mu, g^2) \langle \hat{O}_{LL}(\mu) \rangle, \quad (3.2)$$

where

$$\tilde{C}_{LL}(x_i, x_j, x_\mu, g^2) = \tilde{S}(x_i, x_j) + \frac{\alpha(\mu)}{4\pi} \tilde{D}(x_i, x_j, x_\mu), \quad (3.3)$$

with  $\langle \hat{O}_{LL}(\mu) \rangle$  denoting the matrix element of the operator  $\hat{O}_{LL}$  of eq. (1.2) between external quark states, calculated to  $O(\alpha)$ .  $\langle \hat{O}_{LL}(\mu) \rangle$  can be calculated by

evaluating the diagrams of fig. 3. Note that the diagrams (1), (2) and (3) correspond to the diagrams (e), (c) and (a) respectively. The one-loop diagrams in fig. 3 are gauge dependent and contain infrared as well as ultraviolet divergences. It is crucial to regulate these divergences in the same way as done in the case of the diagrams of fig. 2. We have thus kept the external quark masses whenever necessary and worked in the DR scheme with anticommuting  $\gamma_5$ . Performing the renormalization in the  $\overline{\text{MS}}$  scheme we find

$$\langle \hat{O}_{\text{LL}}(\mu) \rangle = \langle \hat{O}_{\text{LL}} \rangle^{(0)} + \frac{\alpha(\mu)}{4\pi} \sum_k \langle [C_F \hat{1} \otimes \hat{1} A_k^{(1)} + t^a \otimes t^a A_k^{(8)}] \hat{T}_k \rangle, \quad (3.4)$$

where  $k = \text{LL}, 1, 2, 3$ , and

$$A_{\text{LL}}^{(8)} = -6 \ln x_\mu - 5 + 2\xi + (3 + \xi) \ln x_d x_s - 2\xi \frac{1}{x_d - x_s} [x_d \ln x_d - x_s \ln x_s], \quad (3.5)$$

$$A_{\text{LL}}^{(1)} = -3 + 2\xi \ln x_\mu + 2\xi - 2\xi \frac{1}{x_d - x_s} [x_d \ln x_d - x_s \ln x_s], \quad (3.6)$$

$$A_1^{(8)} = -(3 + \xi), \quad (3.7)$$

$$A_2^{(8)} = -2A_3^{(1)} = -(3 + \xi) \frac{m_d m_s}{m_d^2 - m_s^2} \ln \frac{x_d}{x_s}, \quad (3.8)$$

with all remaining coefficients being zero. Inserting (3.4) into (3.2) and comparing with (3.1), we indeed confirm the factorized form of eq. (3.2) and find  $\tilde{D}(x_i, x_j, x_\mu)$  to be

$$\begin{aligned} \tilde{D}(x_i, x_j, x_\mu) &= \frac{N-1}{2N} \{ L^{(8)}(x_i, x_j) + [6 \ln x_\mu + 5] \tilde{S}(x_i, x_j) \} \\ &\quad + \frac{N^2-1}{2N} \left\{ L^{(1)}(x_i, x_j) + \left[ 6 \ln x_\mu \left( x_i \frac{\partial}{\partial x_i} + x_j \frac{\partial}{\partial x_j} \right) + 3 \right] \tilde{S}(x_i, x_j) \right\}. \end{aligned} \quad (3.9)$$

We observe that the coefficient function  $\tilde{C}_{\text{LL}}(x_i, x_j, x_\mu, g^2)$  is gauge independent and does not contain the dependence on the external quark states.

Thus as expected, the gauge dependence and the dependence on the external quarks found in sect. 2 are merely the properties of the matrix elements of local

operators. This assures us that the factorization of short and long distance contributions has been done properly. An additional check of this can be obtained by evaluating the diagrams of figs. 2 and 3 with vanishing external quark masses, but nonvanishing external momenta. This time operators involving  $\not{p}$  appear at intermediate stages of the calculation. The final result for the coefficient function  $C_{LL}$  however turns out to be equal to the one given in eqs. (3.3) and (3.9), as it should.

Comparing eq. (3.9) with eqs. (2.12) and (2.13), we also observe that the coefficient function now contains new terms which were absent in eqs. (2.12) and (2.13). These terms read

$$\Delta\tilde{D}(x_i, x_j, x_\mu) = \left[ R + 6 \left( \frac{N-1}{2N} \right) \ln x_\mu \right] \tilde{S}(x_i, x_j), \quad (3.10)$$

with

$$R = 5 \left( \frac{N-1}{2N} \right) + 3 \left( \frac{N^2-1}{2N} \right). \quad (3.11)$$

As we will see in the next section, the term involving  $\ln x_\mu$  is necessary in order that  $C_{LL}$  obeys the renormalization group equation. The factor  $R$  is particular for the DR scheme. For instance in the dimensional reduction scheme (DRED), or in a scheme with non-anticommuting  $\gamma_5$ , a different expression for  $R$  would be obtained. This is analogous to the situation encountered in ref. [22]. This dependence on the renormalization scheme will be cancelled in the next section after the inclusion of the two-loop anomalous dimension of the operator  $\hat{O}_{LL}$ .

At first sight it could appear that the factorization of short and long distance contributions, and the appearance of a single operator at the end has been imposed by us. Yet this is not the case. Indeed we have explicitly calculated which part of the  $O(\alpha_{QCD})$  corrections belongs (in a given renormalization scheme) to the matrix element of the operator, and which belongs to the coefficient function. Also the reason for only one operator being present at the end is nontrivial. Indeed in general it is possible to generate new operators at the one-loop level, which remain after factorization has been done. This is for instance the case for the  $\Delta S = 1$  hamiltonian discussed in ref. [13]. Then the phenomenon of mixing under renormalization takes place. The case at hand is however different. This is evident from eqs. (3.7) and (3.8) which do not have any  $\mu$ -dependence. Such a  $\mu$ -dependence would be present if a mixing between  $\hat{O}_{LL}$  and the additional operators took place. Equivalently the divergent parts of the diagrams in fig. 3 contain only the operator  $\hat{O}_{LL}$ , i.e. this operator renormalizes without mixing.

As in the previous section, we would like to add a few words of caution. In the process of the calculation of the diagrams (2) and (3) of fig. 3, the following

structures in  $D \neq 4$  dimensions appear

$$S_1 = \gamma_\mu \gamma_\nu \gamma_\lambda (1 - \gamma_5) \otimes \gamma^\mu \gamma^\nu \gamma^\lambda (1 - \gamma_5), \quad (3.12)$$

$$S_2 = \gamma_\mu \gamma_\nu \gamma_\lambda (1 - \gamma_5) \otimes \gamma^\lambda (1 - \gamma_5) \gamma^\nu \gamma^\mu. \quad (3.13)$$

As discussed in ref. [22], it is crucial to evaluate  $S_1$  and  $S_2$  in accordance with the evaluation of the two-loop anomalous dimensions. In the DR scheme used here, the projection of  $S_1$  and  $S_2$  on the physical operator  $\hat{O}_{\text{LL}}$  is

$$S_1 \rightarrow 4(4 - \varepsilon) \hat{O}_{\text{LL}}, \quad S_2 \rightarrow 4(1 - 2\varepsilon) \hat{O}_{\text{LL}}, \quad (3.14)$$

with  $D = 4 - 2\varepsilon$ . The  $O(\varepsilon)$  terms in eq. (3.14) have to be retained in order to obtain the correct results.

#### 4. Renormalization group analysis

##### 4.1. PRELIMINARIES

The renormalization group equation for the Wilson coefficient function of the operator  $\hat{O}_{\text{LL}}$  reads

$$\left[ \mu \frac{\partial}{\partial \mu} + \beta(g) \frac{\partial}{\partial g} - \gamma_m(g) \sum_k m_k \frac{\partial}{\partial m_k} - \gamma(g) \right] \tilde{C}_{\text{LL}}(x_i, x_j, x_\mu, g^2) = 0, \quad (4.1)$$

where  $\gamma_m(g)$  and  $\gamma(g)$  are the anomalous dimensions of the mass operator and of the operator  $\hat{O}_{\text{LL}}$  respectively. We have left out the derivative with respect to the gauge parameter, since we have explicitly demonstrated in the previous section, that the coefficient function  $C_{\text{LL}}$  is gauge independent.

The functions  $\beta(g)$ ,  $\gamma_m(g)$  and  $\gamma(g)$  have the following expansions in  $g$ :

$$\beta(g) = -\beta_0 \frac{g^3}{16\pi^2} - \beta_1 \frac{g^5}{(16\pi^2)^2} + \dots, \quad (4.2)$$

$$\gamma_m(g) = \gamma_m^{(0)} \frac{g^2}{16\pi^2} + \gamma_m^{(1)} \frac{g^4}{(16\pi^2)^2} + \dots, \quad (4.3)$$

$$\gamma(g) = \gamma^{(0)} \frac{g^2}{16\pi^2} + \gamma^{(1)} \frac{g^4}{(16\pi^2)^2} + \dots, \quad (4.4)$$

where

$$\beta_0 = \frac{1}{3}(11N - 2f), \quad \beta_1 = \frac{34}{3}N^2 - \frac{10}{3}Nf - 2C_F f, \quad (4.5)$$

$$\gamma_m^{(0)} = 6C_F, \quad \gamma_m^{(1)} = C_F \left[ 3C_F + \frac{97}{3}N - \frac{10}{3}f \right], \quad (4.6)$$

$$\gamma^{(0)} = 6 \frac{N-1}{N}, \quad \gamma^{(1)} = \frac{N-1}{2N} \left[ -21 + \frac{57}{N} - \frac{19}{3}N + \frac{4}{3}f \right]. \quad (4.7)$$

The coefficients given in eqs. (4.5) and (4.6), as well as  $\gamma^{(0)}$ , are well known. However the two-loop anomalous dimension  $\gamma^{(1)}$  of the operator  $\hat{O}_{LL}$  is new. It has been obtained on the basis of our previous paper [22] by noticing that the flavour structure of  $\hat{O}_{LL}$  implies that the anomalous dimension of  $\hat{O}_{LL}$  is simply equal to the one of the operator  $\hat{O}_+$  of ref. [22].  $\gamma^{(1)}$  depends on the renormalization scheme. In accordance with the calculation of the previous sections, the value in eq. (4.7) is given in the DR scheme.  $\gamma^{(1)}$  in other schemes can be found in refs. [22, 23].

Inserting eq. (3.3) into eq. (4.1), we verify that the coefficient function found in the previous section satisfies the renormalization group equation. It is also clear from this exercise that the first  $\ln x_\mu$  in eq. (3.9) describes the evolution of the operator  $\hat{O}_{LL}$  (it is related to  $\gamma^{(0)}$ ), whereas the second  $\ln x_\mu$  describes the running of the internal quark masses.

#### 4.2. EVOLUTION TO LOW ENERGIES

Since  $\mu$  in eq. (3.9) is arbitrary let us first set  $\mu = M_W$ . This choice removes the  $\ln x_\mu$  terms and normalizes the running top quark mass at  $\mu = M_W$ . We will later discuss other choices which should give of course the same physical results.

In what follows, it will be useful to use the unitarity of the CKM matrix and concentrate on the term proportional to  $\lambda_1^2$ . The effective hamiltonian entering eq. (3.2) reduces to the following expression

$$(H_{\text{eff}})_{tt} = \frac{G_F^2}{16\pi^2} M_W^2 \lambda_1^2 C_{LL}(x_t, \bar{g}^2(M_W)) \hat{O}_{LL}(M_W), \quad (4.8)$$

where

$$C_{LL}(x_t, \bar{g}^2(M_W)) = S(x_t) + \frac{\alpha(M_W)}{4\pi} D(x_t). \quad (4.9)$$

Since the Wilson coefficient function of  $\hat{O}_{LL}$  has been found to be independent of the external states, we have dropped the reference to the latter and have written

eq. (4.8) in operator form. The expression for  $D(x_t)$  reads

$$D(x_t) = W(x_t) + RS(x_t), \quad (4.10)$$

where  $R$  is given in eq. (3.11), and

$$W(x_t) = L(x_t, x_t) - 2L(x_t, x_u) + L(x_u, x_u), \quad (4.11)$$

with  $L(x_i, x_j)$  defined by

$$L(x_i, x_j) = \left( \frac{N-1}{2N} \right) L^{(8)}(x_i, x_j) + \left( \frac{N^2-1}{2N} \right) L^{(1)}(x_i, x_j). \quad (4.12)$$

The expression in eq. (4.9) represents the initial condition for the Wilson coefficient function at the scale  $M_w$ . It is not equal to the value obtained in the free field theory. The correction represented by the second term in (4.9) is a calculable function of  $m_t$ . This function given in eq. (4.10) has two terms. The first one does not depend on the way the operator is renormalized, but the second term does. Also  $\hat{O}_{LL}(M_w)$  depends on the renormalization scheme and this dependence precisely cancels the one of the second term in eq. (4.10).

In order to obtain the generalization of eq. (1.1) beyond the leading order, we have to re-express  $\hat{O}_{LL}(M_w)$  in terms of  $\hat{O}_{LL}(\mu)$ , with  $\mu$  now being some low energy scale

$$\hat{O}_{LL}(M_w) = \exp \left[ - \int_{\bar{g}(\mu)}^{\bar{g}(M_w)} dg' \frac{\gamma(g')}{\beta(g')} \right] \hat{O}_{LL}(\mu). \quad (4.13)$$

This is simply the evolution of  $\hat{O}_{LL}$  from  $M_w$  down to  $\mu$ , which is governed by a renormalization group equation similar to (4.1). This evolution can be done in a massless theory, because the top quark has been integrated out, and hence  $m_t$  is only contained in the initial condition (4.9). In any case we work in a mass-independent renormalization scheme, and consequently, as seen in eqs. (4.2) to (4.7), the  $\beta$ -function and the anomalous dimensions  $\gamma_m$  and  $\gamma$  are independent of quark masses. In a mass-dependent renormalization scheme this would no longer be the case, but then also the calculation of finite terms would be different to that presented here so that the same final result would be obtained.

It should also be stressed that we evolve only  $\hat{O}_{LL}(M_w)$  down to lower scales. This evolution does not affect the heavy quark masses which are contained in  $C_{LL}(x_t, \bar{g}^2(M_w))$ . Consequently at all stages the top quark mass entering  $D(x_t)$  is the running top quark mass evaluated at  $M_w$ .

Inserting eqs. (4.2) and (4.4) into (4.13) and expanding the exponential in powers of  $\bar{g}^2$  we find

$$\hat{O}_{LL}(M_w) = \left[ 1 + \frac{\alpha(M_w) - \alpha(\mu)}{4\pi} Z \right] \left[ \frac{\alpha(M_w)}{\alpha(\mu)} \right]^{d^{(0)}} \hat{O}_{LL}(\mu), \quad (4.14)$$



where

$$Z = \frac{\gamma^{(1)}}{2\beta_0} - \frac{d^{(0)}}{\beta_0}\beta_1, \quad d^{(0)} = \frac{\gamma^{(0)}}{2\beta_0}. \quad (4.15)$$

Inserting eq. (4.14) into (4.8), we can rewrite  $(H_{\text{eff}})_{tt}$  in the desired form

$$(H_{\text{eff}})_{tt} = \frac{G_F^2}{16\pi^2} M_W^2 \lambda_t^2 \tilde{\eta}_2(x_t) S(x_t) [\hat{O}_{LL}] \quad (4.16)$$

where

$$\tilde{\eta}_2(x_t) = [\alpha(M_W)]^{d^{(0)}} \left[ 1 + \frac{\alpha(M_W)}{4\pi} (Y(x_t) + R + Z) \right], \quad (4.17)$$

$$[\hat{O}_{LL}] \equiv [\alpha(\mu)]^{-d^{(0)}} \left[ 1 - \frac{\alpha(\mu)}{4\pi} Z \right] \hat{O}_{LL}(\mu), \quad Y(x_t) = \frac{W(x_t)}{S(x_t)}. \quad (4.18)$$

The coefficient of  $\alpha(M_W)$  in eq. (4.17) does not depend on the renormalization scheme, since such a dependence cancels in the sum  $R + Z$ . It should also be stressed that both  $\tilde{\eta}_2$  and  $[\hat{O}_{LL}]$  do not depend on  $\mu$ . They are essentially the generalizations of eqs. (1.4)–(1.6) beyond the leading order, except that the distinction between effective theories of different flavour in the process of the evolution to lower scales has not yet been incorporated into eq. (4.17). We will do this in the next section, where the numerical evaluation of the corrections will be presented.

## 5. Basic results

### 5.1. PRELIMINARIES

In this section we will present our final expressions for the QCD factors  $\eta_{2K}$  and  $\eta_{2B}$ , relevant for the K-meson and B-meson systems. There are many different aspects of these results, and we have to proceed in a systematic fashion. For pedagogical reasons we begin by giving the results of calculations in which, as in the previous section, (i) the evolution of the operator  $\hat{O}_{LL}$  down to low energies starts at  $\mu = M_W$ , and (ii) the top quark mass used is defined to be  $m_t \equiv \bar{m}_t(M_W)$ . After a discussion of the limiting cases  $m_t \ll M_W$  and  $m_t \gg M_W$ , which will give us insight into the structure of the dominant contributions, and will test our formulae, we will investigate other choices for the initial scale of the operator  $\hat{O}_{LL}$ , and other definitions of the top quark mass. We will find that (i) the QCD factors  $\eta_2$  do *not* depend on the initial scale of the evolution of the operator  $\hat{O}_{LL}$  down to low energies, but (ii) they do *depend* on the definition of the top quark mass. In

particular we will study the case  $m_t^* \equiv \overline{m}_t(m_t)$ . Denoting the resulting QCD factors by  $\eta_2^*$ , we note the important equation:

$$\eta_2^*(x_t^*)S(x_t^*) = \eta_2(x_t)S(x_t), \quad (5.1)$$

with  $x_t^*$  and  $x_t$  related through eq. (5.33). We will see that for large  $m_t$  the functions  $\eta_2^*$  and  $\eta_2$  must differ considerably in order to compensate for  $S(x_t^*) \neq S(x_t)$ . Eq. (5.1) demonstrates that the final result for the physical quantities, obtained from  $H_{\text{eff}}$ , does not depend on the definition of the top quark mass used in the actual calculations. We will illustrate this explicitly below. Finally we present some phenomenological implications of our results.

## 5.2. $\eta_2$ FOR THE K-SYSTEM

Including the distinction between different effective theories in the process of evolution from  $M_W$  down to  $\mu < m_c$ , we find in a straightforward way

$$(H_{\text{eff}})_{tt} = \frac{G_F^2}{16\pi^2} M_W^2 \lambda_t^2 \eta_{2K}(x_t) S(x_t) [\hat{O}_{LL}], \quad (5.2)$$

where

$$\begin{aligned} \eta_{2K}(x_t) &= [\alpha_3(m_c)]^{6/27} \left[ \frac{\alpha_4(m_b)}{\alpha_4(m_c)} \right]^{6/25} \left[ \frac{\alpha_5(M_W)}{\alpha_5(m_b)} \right]^{6/23} \\ &\times \left[ 1 + \frac{\alpha_5(M_W)}{4\pi} (Y(x_t) + R + Z_5) \right. \\ &\quad \left. + \frac{\alpha_4(m_b)}{4\pi} (Z_4 - Z_5) + \frac{\alpha_3(m_c)}{4\pi} (Z_3 - Z_4) \right], \end{aligned} \quad (5.3)$$

$$[\hat{O}_{LL}] \equiv [\alpha_3(\mu)]^{-2/9} \left[ 1 - \frac{\alpha_3(\mu)}{4\pi} Z_3 \right] \hat{O}_{LL}(\mu). \quad (5.4)$$

Here

$$\alpha_f(Q) = \frac{4\pi}{\beta_0 \ln Q^2/\Lambda_f^2} \left[ 1 - \frac{\beta_1}{\beta_0^2} \frac{\ln \ln Q^2/\Lambda_f^2}{\ln Q^2/\Lambda_f^2} \right], \quad (5.5)$$

with  $\beta_0$  and  $\beta_1$  given in eq. (4.5). We have dropped the subscript  $\overline{\text{MS}}$ , in order to simplify the notation. Demanding the continuity of  $\alpha_f(Q)$  in the form

$$\alpha_3(m_c) = \alpha_4(m_c), \quad \alpha_4(m_b) = \alpha_5(m_b), \quad (5.6)$$

gives relations between the various values for  $\Lambda_f$ . Once one of the  $\Lambda_f$  is determined by experiment, the remaining ones can be found from these relations. In our analysis, we calculated the latter numerically from (5.5) and (5.6). It turns out that to a reasonable approximation (10–20%) the leading order relations

$$\Lambda_4 = \Lambda_3 \left[ \frac{\Lambda_3}{m_c} \right]^{2/25}, \quad \Lambda_5 = \Lambda_4 \left[ \frac{\Lambda_4}{m_b} \right]^{2/23} \quad (5.7)$$

remain valid. In our phenomenological analysis we will denote  $\Lambda_4 \equiv \Lambda_{\overline{\text{MS}}}$ . The quantities  $R$  and  $Z_f$  are defined in eqs. (3.11) and (4.15) respectively.

Finally, but most importantly, the function  $Y(x_t)$  is given by

$$Y(x_t) = \frac{W(x_t)}{S(x_t)} \quad \text{with} \quad W(x_t) = \left( \frac{N-1}{2N} \right) W^{(8)}(x_t) + \left( \frac{N^2-1}{2N} \right) W^{(1)}(x_t), \quad (5.8)$$

and  $S(x_t)$  being defined in eq. (2.4). The functions  $W^{(8)}(x_t)$  and  $W^{(1)}(x_t)$  have the explicit form

$$\begin{aligned} W^{(8)}(x_t) = & \frac{8}{3} \frac{\pi^2}{x_t} - \frac{64 - 68x_t - 17x_t^2 + 11x_t^3}{4(1-x_t)^2} + \frac{1}{2(1-x_t)^3} \\ & \times \left[ (32 - 68x_t + 32x_t^2 - 28x_t^3 + 3x_t^4) \ln x_t + 9x_t^3 \ln^2 x_t \right. \\ & \left. + \frac{4}{x_t} (8 - 32x_t + 44x_t^2 - 19x_t^3) I_{1,1-x_t} - 4x_t^2 (2 - 8x_t + 8x_t^2 - x_t^3) I_{x_t, x_t-1} \right], \quad (5.9) \end{aligned}$$

$$\begin{aligned} W^{(1)}(x_t) = & - \frac{x_t(4 - 39x_t + 168x_t^2 + 11x_t^3)}{4(1-x_t)^3} \\ & - \frac{3x_t}{(1-x_t)^2} \left[ 2(4 - 6x_t - x_t^2) I_{1,1-x_t} - (1-x_t)(8 - 4x_t - x_t^2) I_{x_t, x_t-1} \right] \\ & - \frac{3x_t}{2(1-x_t)^4} \left[ (4 - 24x_t + 36x_t^2 + 7x_t^3 + x_t^4) \ln x_t \right. \\ & \left. - 2(4 - 10x_t + 14x_t^2 + x_t^3) \ln^2 x_t \right]. \quad (5.10) \end{aligned}$$

The functions  $I_{1,1-x_t}$  and  $I_{x_t, x_t-1}$  are defined in appendix A. Despite appearances there are no singularities at  $x_t = 0$  and  $x_t = 1$ , as one can convince oneself by using the properties of the  $I$ -functions given in appendix A. In fact  $W^{(8)}(x_t)$  and  $W^{(1)}(x_t)$  vanish for  $x_t = 0$  in accordance with the GIM mechanism. Further properties of these formulae are discussed below.

The formula (5.3) represents the generalization of the leading order expression given in eq. (1.4). The following remarks should be made:

- (a) The  $\alpha_f$  used in the leading order are given in eq. (1.3), whereas eq. (5.5) should be used in eq. (5.3). This, as we will see, gives a small suppression of  $\eta_2$  for the same value of  $\Lambda_{\overline{\text{MS}}}$ .
- (b) The  $Z_f$  are renormalization prescription dependent, but the differences  $Z_4 - Z_5$  and  $Z_3 - Z_4'$  are free from this dependence. This is evident from the analysis of ref. [22], where  $Z_f$  have been calculated in various schemes.
- (c) The scheme dependence of  $Z_5$  is cancelled by the one of  $R$ , so that the sum  $Y(x_t) + R + Z_5$  is scheme independent except for a redefinition of the coupling constant.
- (d) The final result for  $\eta_{2K}$  is renormalization scheme independent (i.e. modulo higher order corrections the numerical values for  $\eta_{2K}$  do not depend on the scheme) and does not depend on  $\mu$ . It depends however on  $\Lambda_{\overline{\text{MS}}}$ ,  $m_t$  and very weakly on  $m_b$  and  $m_c$ . The dependence on  $\Lambda_{\overline{\text{MS}}}$  and  $m_t$  is given below.
- (e) Also the formula for  $B_K$  gets modified,

$$B_K = B_K(\mu) [\alpha_3(\mu)]^{-2/9} \left[ 1 - \frac{\alpha_3(\mu)}{4\pi} Z_3 \right], \quad (5.11)$$

with  $B_K(\mu)$  representing the result of a nonperturbative evaluation of the relevant hadronic matrix element (see eq. (1.6)). The new feature is that the factor multiplying  $B_K(\mu)$  is via  $Z_3$  renormalization scheme dependent. Consequently in order to evaluate  $B_K$  one has to make sure that the nonperturbative calculation of  $B_K(\mu)$  has been performed in the same renormalization scheme. Note that in contrast to eq. (1.5),  $\alpha_3(\mu)$  is given by eq. (5.5).

Before presenting the numerical analysis of eq. (5.3), let us recall that in the leading order  $\eta_{2K}$ , as given in eq. (1.4), has a very weak dependence on  $\Lambda_{\text{QCD}}$ . Taking  $m_c = 1.35$  GeV,  $m_b = 4.8$  GeV and  $M_W = 80$  GeV one finds

$$(\eta_2^K)_{\text{Leading}} = \begin{cases} 0.604 & \text{for } \Lambda_{\overline{\text{MS}}} = 100 \text{ MeV} \\ 0.616 & \text{for } \Lambda_{\overline{\text{MS}}} = 200 \text{ MeV} \\ 0.624 & \text{for } \Lambda_{\overline{\text{MS}}} = 300 \text{ MeV} \end{cases} \quad (5.12)$$

It is instructive to investigate the effect of the two-loop expression for  $\alpha_f(Q)$ , as given in eq. (5.5), on the factor in front of the square bracket in eq. (5.3), i.e. eq.

TABLE 1  
The values for  $\eta_{2K}$ ,  $\eta_{2B}$  and  $\bar{\eta}_{2B}$  as functions of  $\bar{m}_t(M_W)$  for different values of  $\Lambda_4$

$\eta_2(m_t)$	$m_t$ [GeV]	$\Lambda_4 = 100$ MeV	$\Lambda_4 = 200$ MeV	$\Lambda_4 = 300$ MeV
$(\eta_{2K})_{LO}$	—	0.604	0.616	0.624
$\eta_{2K}(m_t)$	70	0.582	0.592	0.598
	90	0.564	0.572	0.576
	110	0.550	0.556	0.559
	130	0.538	0.542	0.544
	150	0.527	0.530	0.531
	200	0.505	0.505	0.504
	250	0.487	0.484	0.482
	300	0.470	0.466	0.462
$(\eta_{2B})_{LO}$	—	0.571	0.588	0.599
$\eta_{2B}(m_t)$	70	0.547	0.562	0.571
	90	0.530	0.543	0.551
	110	0.517	0.528	0.534
	130	0.506	0.515	0.520
	150	0.496	0.504	0.508
	200	0.475	0.480	0.483
	250	0.458	0.460	0.461
	300	0.443	0.443	0.442
$(\bar{\eta}_{2B})_{LO}$	—	0.875	0.856	0.842
$\bar{\eta}_{2B}(m_t)$	70	0.905	0.892	0.882
	90	0.878	0.863	0.851
	110	0.857	0.839	0.826
	130	0.838	0.819	0.806
	150	0.822	0.802	0.787
	200	0.789	0.765	0.749
	250	0.761	0.735	0.717
	300	0.736	0.708	0.688

(1.4). One finds

$$(\eta_2^K)_{\text{Leading}}^{2\text{-loop } \alpha} = \begin{cases} 0.586 & \text{for } \Lambda_{\overline{MS}} = 100 \text{ MeV} \\ 0.597 & \text{for } \Lambda_{\overline{MS}} = 200 \text{ MeV} , \\ 0.603 & \text{for } \Lambda_{\overline{MS}} = 300 \text{ MeV} \end{cases} \quad (5.13)$$

i.e. a 3% suppression with respect to the leading order result of eq. (5.12).

The complete result for  $\eta_{2K}$  as a function of  $m_t(M_W)$  is given in table 1 and fig. 4. For convenience of the reader, we have also included the leading order values for  $\eta_2$  in table 1. At this stage we would like to remark that in the case of  $m_t \gg M_W$  one could ask whether the use of a normalization point much lower than the actual experimental value of the quark mass is very physical [24]. In spite

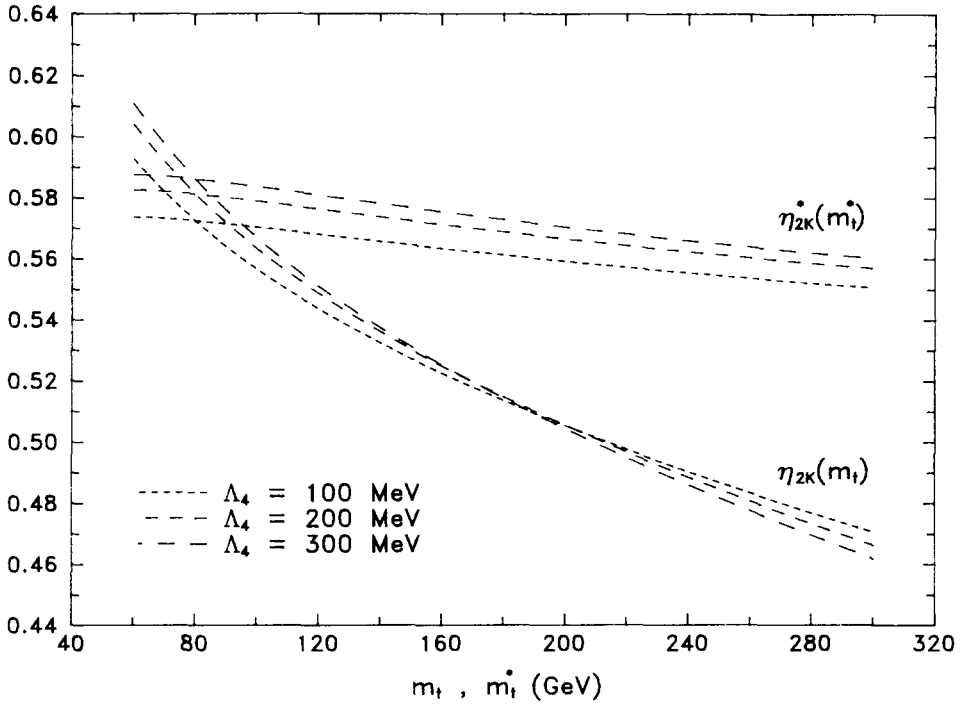


Fig. 4.  $\eta_{2K}(m_t)$  given in eq. (5.3) and  $\eta_{2K}^*(m_t^*)$  as functions of  $m_t$  and  $m_t^*$  for different values of  $\Lambda_4$ .

of this it should be stressed that such a procedure is fully mathematically consistent as is evident from the discussion of subsect. 4.2. The following observations can be made on the basis of fig. 4 and table 1:

- (i)  $\eta_{2K}$  decreases substantially with increasing values of  $m_t$ , but is rather weakly dependent on  $\Lambda_4$ .
- (ii) For  $m_t \approx M_W$  the effect of next-to-leading order corrections is small, but becomes sizeable for  $200 \text{ GeV} \leq m_t \leq 300 \text{ GeV}$ , i.e. a 20–25% reduction of  $\eta_{2K}$  compared to the leading order values given in eq. (5.12).
- (iii) This decrease can be mainly attributed to  $W^{(1)}(x_t)$  of eq. (5.10), and as discussed in subsect. 5.5, originates in the QCD corrections to box diagrams with two fictitious Higgs exchanges.
- (iv) Whereas  $Y(x_t) < 0$ , the sum  $R + Z_5$  is positive, which slightly compensates the decrease of  $\eta_{2K}$  due to  $Y(x_t)$ . Equivalently since  $R + Z_5 \approx 4$  and  $\alpha_5(M_W)/4\pi \approx 0.01$ , this term cancels roughly the decrease of  $\eta_{2K}$  due to two-loop effects in  $\alpha$  (see eq. (5.13)), leaving  $Y(x_t)$  as the net effect of the next-to-leading order corrections.

We will elaborate on the size of the next-to-leading order corrections in subsect. 5.8.

5.3.  $\eta_2$  FOR THE B-SYSTEM

The analysis of  $\eta_{2B}$  proceeds along the same lines except that  $\mu = O(m_b)$  and

$$\hat{O}_{LL} = (\bar{b}d)_{V-A}(\bar{b}d)_{V-A}. \quad (5.14)$$

If the external b-quark mass is neglected, one again finds eq. (5.2) with  $\eta_{2K}$  replaced by

$$\eta_{2B}(x_t) = [\alpha_s(M_W)]^{6/23} \left[ 1 + \frac{\alpha_s(M_W)}{4\pi} (Y(x_t) + R + Z_5) \right], \quad (5.15)$$

$$[\hat{O}_{LL}] \equiv [\alpha_s(\mu)]^{-6/23} \left[ 1 - \frac{\alpha_s(\mu)}{4\pi} Z_5 \right] \hat{O}_{LL}(\mu). \quad (5.16)$$

Correspondingly

$$B_B = B_B(\mu) [\alpha_s(\mu)]^{-6/23} \left[ 1 - \frac{\alpha_s(\mu)}{4\pi} Z_5 \right], \quad (5.17)$$

is renormalization group invariant.

Our definition of  $\eta_{2B}$  is in accordance with  $\eta_{2K}$ , but differs from the one used in the literature. It is important to emphasize this difference. The usual practice in the case of  $B^0-\bar{B}^0$  mixing is to choose  $\mu = m_b$  and include the factors multiplying  $\hat{O}_{LL}(\mu)$  in  $\eta_{2B}$ . Denoting by  $\bar{\eta}_{2B}$  the resulting QCD factor we find

$$\bar{\eta}_{2B}(x_t) = \left[ \frac{\alpha_s(M_W)}{\alpha_s(m_b)} \right]^{6/23} \left[ 1 + \frac{\alpha_s(M_W)}{4\pi} (Y(x_t) + R + Z_5) - \frac{\alpha_s(m_b)}{4\pi} Z_5 \right]. \quad (5.18)$$

In the leading order eq. (5.18) reduces to the expression used in the literature

$$(\bar{\eta}_{2B})_{\text{Leading}} = \left[ \frac{\alpha_s(M_W)}{\alpha_s(m_b)} \right]^{6/23}, \quad (5.19)$$

whereas (5.15) gives

$$(\eta_{2B})_{\text{Leading}} = [\alpha_s(M_W)]^{6/23}. \quad (5.20)$$

For typical values of  $A_{\text{QCD}}$ ,  $(\bar{\eta}_{2B})_{\text{Leading}} \approx 1.5(\eta_{2B})_{\text{Leading}}$ , which is compensated by the difference between  $B_B$  and  $B_B(m_b)$ .

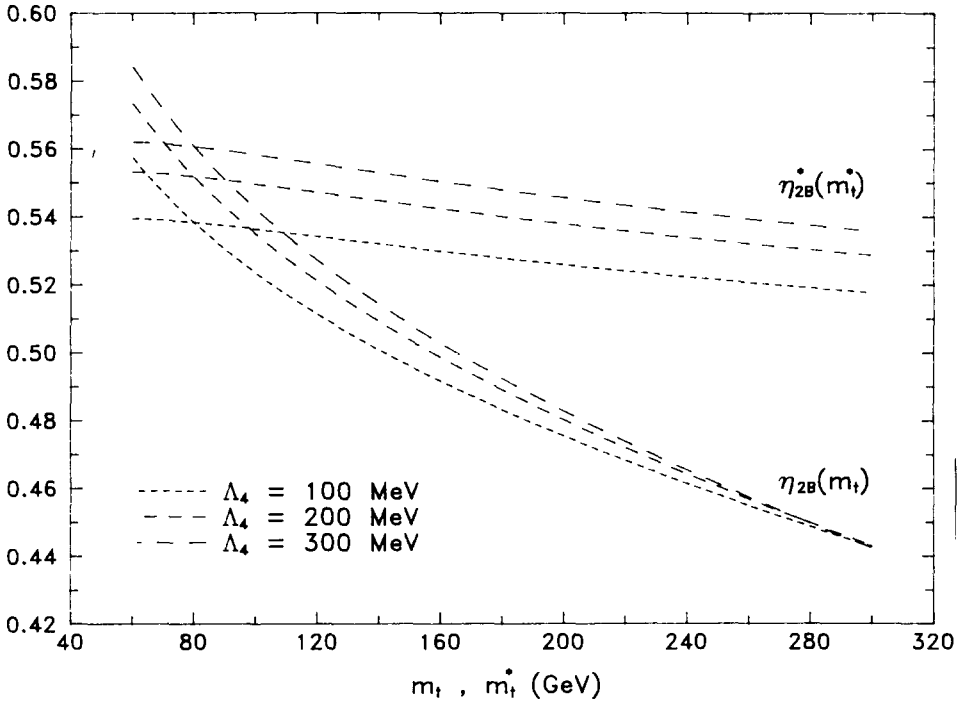


Fig. 5.  $\eta_{2B}(m_t)$  given in eq. (5.15) and  $\eta_{2B}^*(m_t^*)$  as functions of  $m_t$  and  $m_t^*$  for different values of  $\Lambda_4$ .

It is clear that the final result for  $B^0-\bar{B}^0$  mixing does not depend on the definition of  $\eta_{2B}$ . However it is crucial to remember which definition has been used, when the values for  $B_B$  or  $B_B(m_b)$  are incorporated in the analysis. The definitions given in eqs. (5.15) and (5.16) have the advantage that both  $\eta_{2B}$  and  $B_B$  do not depend on the renormalization scheme. This is not the case for  $\bar{\eta}_{2B}$  and  $B_B(m_b)$ . The expression given in eq. (5.18) corresponds to the  $\overline{MS}$  scheme and in order to obtain a renormalization-scheme independent result for  $B^0-\bar{B}^0$  mixing,  $B_B(m_b)$  should be extracted in the same scheme. For completeness, we give the numerical results for both  $\eta_{2B}$  and  $\bar{\eta}_{2B}$ . They are collected in table 1, as well as figs. 5 and 6. The comments made in connection with  $\eta_{2K}$  apply also here.

#### 5.4. SMALL $m_t$ -BEHAVIOUR

Although the case  $m_t \ll M_W$  is excluded by experiment, it is instructive to compare our results with the formulae of Gilman and Wise [8] obtained for small values of  $m_t$

$$(H_{\text{eff}})_{tt}^{\text{GW}} = \frac{G_F^2}{16\pi^2} \lambda_t^2 \hat{O}_{LL} J_{tt}, \quad (5.21)$$



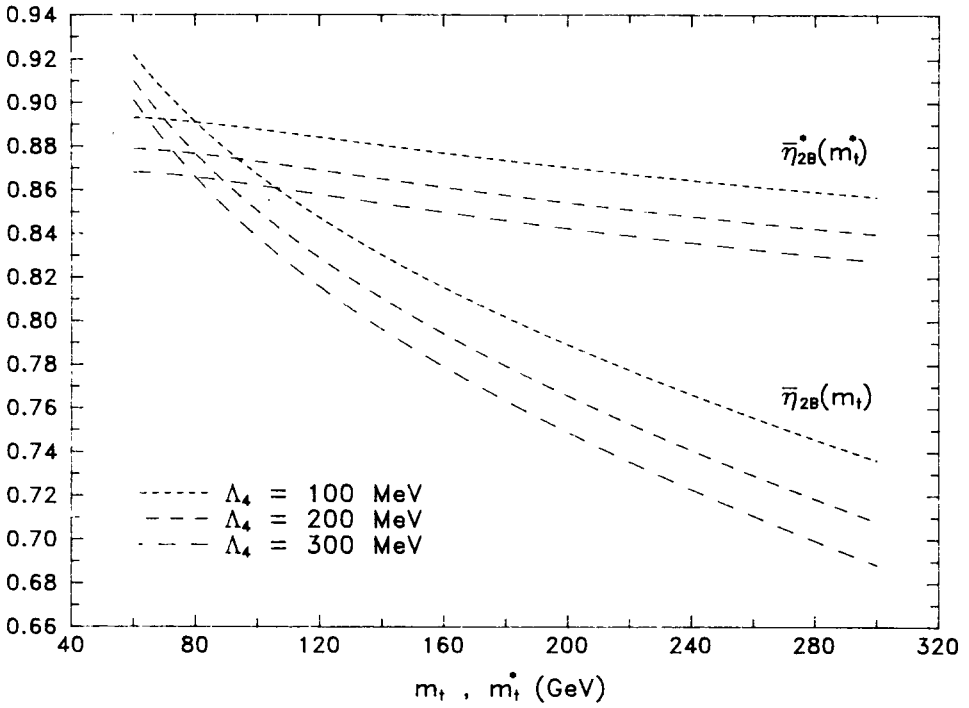


Fig. 6.  $\bar{\eta}_{2B}(m_t)$  given in eq. (5.18) and  $\bar{\eta}_{2B}^*(m_t^*)$  as functions of  $m_t$  and  $m_t^*$  for different values of  $\Lambda_4$ .

where

$$J_{tt} = m_t^{\diamond^2} \left[ \frac{\alpha_3(m_c)}{\alpha_3(\mu)} \right]^{\gamma_+/2\beta_3} \left[ \frac{\alpha_4(m_b)}{\alpha_4(m_c)} \right]^{\gamma_+/2\beta_4} \left[ \frac{\alpha_5(m_t)}{\alpha_5(m_b)} \right]^{\gamma_+/2\beta_5} \\ \times \sum_{\sigma, \tau = \pm} C_{\sigma\tau} \left[ \frac{\alpha_6(M_W)}{\alpha_6(m_t)} \right]^{(\gamma_\sigma + \gamma_\tau)/2\beta_6}, \quad (5.22)$$

with\*

$$\gamma_\pm = \pm \frac{6}{N}(N \mp 1), \quad \beta_f = \frac{1}{3}(11N - 2f), \quad (5.23)$$

$$C_{++} = \frac{1}{4}(N + 3), \quad C_{--} = \frac{1}{4}(N - 1) = -C_{+-}, \quad (5.24)$$

and

$$m_t^{\diamond^2} = m_t^2 \left[ \frac{\alpha_6(m_t)}{\alpha_6(\mu)} \right]^{\gamma_m^{(0)}/\beta_6}. \quad (5.25)$$

\*  $\gamma_\pm$  are the anomalous dimensions of the diagonal operators  $\hat{O}_+$  and  $\hat{O}_-$  present in the  $\Delta S = 1$  hamiltonian [5, 22].

We also note the property

$$\sum_{\sigma, \tau} C_{\sigma\tau} = 1. \quad (5.26)$$

Expanding eq. (5.22) in  $\alpha$ , and dropping the flavour dependence for simplicity, we find

$$J_{tt} = m_t^2 \left[ 1 - \frac{\alpha}{4\pi} \left( \gamma_m^{(0)} \ln \frac{m_t^2}{\mu^2} + \frac{\gamma_+}{2} \ln \frac{m_t^2}{\mu^2} + \gamma_+ \ln \frac{M_W^2}{m_t^2} + \dots \right) \right], \quad (5.27)$$

where the dots stand for nonlogarithmic terms. This formula is supposed to be valid for  $M_W^2 \gg m_t^2 \gg \mu^2$ .

In order to compare (5.27) with our results, we take the limit  $x_t \rightarrow 0$  in eq. (3.3) and drop the constant terms to find  $M_W^2 C_{LL}(x_t, x_\mu, g^2) \rightarrow J_{tt}$ , where  $C_{LL}(x_t, x_\mu, g^2)$  is obtained from (3.3) after inclusion of the GIM mechanism, i.e. we verify Gilman and Wise's result of eq. (5.27). This is another test of our calculation. Three comments should be made:

(i) The logarithm multiplying  $\gamma_m^{(0)}$  is  $\ln m_t^2/\mu^2$  and not  $\ln x_\mu$  as given in eq. (3.9). Yet our result in (3.9) agrees with (5.27), because there is an additional logarithm  $\ln x_t$  present in  $L^{(1)}(x_i, x_j)$  which compensates for this difference. We will return to this in subsect. 5.6.

(ii) Setting  $\mu = m_t$  in eq. (5.27), we observe that the evolution from  $M_W$  down to  $m_t$  (for not too small  $m_t$ ) is "effectively" twice as fast as from  $m_t$  down to  $\mu \ll m_t$ . This can be understood as follows. Whereas for  $m_t^2 \ll \mu^2 \ll M_W^2$ , the bilocal structure given in fig. 7 with two operator vertices is responsible for the evolution, for  $\mu^2 \ll m_t^2$  only the local operator  $\hat{O}_{LL}$  with anomalous dimension  $\gamma^{(0)} = \gamma_+$ , considered by us, is present. For  $m_t$  not too small, the evolution from  $M_W$  down to  $m_t$  is dominated by the  $(+, +)$  term in eq. (5.22) which corresponds to the diagram of fig. 7 with two  $\hat{O}_+$  operators. The effective anomalous dimension is in this range therefore twice as large as in the case of the local operator  $\hat{O}_{LL}$ . As we have seen our result incorporates this feature.

(iii) The evolution from  $M_W$  down to  $m_t$ , given by eq. (5.22), is in an exponentiated form, whereas in our analysis we did not exponentiate  $\ln x_t$ . Moreover there are also contributions from the  $\hat{O}_-$  operator which are clearly not present in our

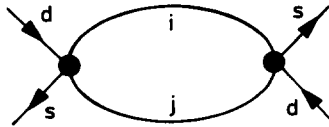


Fig. 7. The leading bilocal operator relevant for the evaluation of  $\eta_1$ .

approach. We would therefore have to modify our analysis appropriately, had we considered a very small  $m_t$ , or discussed the charm contribution, i.e. the coefficients  $\eta_1$  and  $\eta_3$  of eq. (1.1). We will return to this in a forthcoming publication. At the time being it is however instructive to check for which values of  $m_t$  the exponentiation of  $\ln x_t$  and the presence of the operators  $\hat{O}_-$  do not matter. In order to simplify matters we again drop the flavour dependence in eq. (5.22) and compare

$$J_{tt} = m_t^{\diamond^2} \left[ \frac{\alpha_5(m_t)}{\alpha_5(\mu)} \right]^{\gamma_+/2\beta_5} \sum_{\sigma, \tau = \pm} C_{\sigma\tau} \left[ \frac{\alpha_6(M_W)}{\alpha_6(m_t)} \right]^{(\gamma_\sigma + \gamma_\tau)/2\beta_6}, \quad (5.28)$$

with eq. (5.27), where we exponentiated the first two logarithms which describe the evolution from  $m_t$  down to  $\mu$  and set  $\alpha = \alpha_6(m_W)$ . We find that down to  $m_t = 20$  GeV, eq. (5.27) is a very good approximation of (5.28), i.e. exponentiation of  $\ln x_t$  and the presence of  $\hat{O}_-$  do not matter. Only for  $m_t < 20$  GeV do these effects need to be taken into account.

### 5.5. LARGE $m_t$ -BEHAVIOUR

For large  $m_t$  the coefficient function  $C_{LL}$  is dominated by the diagrams with two fictitious Higgs exchanges. Therefore symbolically  $W(x_t) \rightarrow HH(x_t)$ , with  $W(x_t)$  given in eq. (5.8). The leading contributions coming from  $WH$  and  $WW$  exchanges are of order  $O(\ln^2 x_t)$  and  $O((1/x_t)\ln^2 x_t)$  respectively. For the following discussion we give in table 2 the asymptotic expressions for all diagrams separately. From

TABLE 2  
Large  $m_t$  behaviour of the leading order box diagram and the  $O(\alpha)$  diagrams contributing to  $W(x_t)$

$S(x_t)$	$\frac{1}{4}x_t$
$HH_a(x_t, x_t)$	$-\frac{1}{2}[6 - \pi^2 + 3 \ln x_t]x_t$
$HH_b(x_t, x_t)$	$-3x_t$
$HH_c(x_t, x_t)$	$\frac{3}{4}x_t$
$HH_d(x_t, x_t)$	$\frac{1}{6}[15 - \pi^2]x_t$
$HH^{(8)}(x_t, x_t)$	$-\frac{1}{12}[33 - 4\pi^2 + 18 \ln x_t]x_t$
$HH_e(x_t, x_t)$	$\frac{3}{4}x_t$
$HH_f(x_t, x_t)$	$[7 - \pi^2 - 3 \ln x_t]x_t$
$HH_g(x_t, x_t)$	$-\frac{1}{2}[10 - \pi^2 - 3 \ln x_t]x_t$
$HH^{(1)}(x_t, x_t)$	$\frac{1}{4}[11 - 2\pi^2 - 6 \ln x_t]x_t$

these expressions one easily deduces

$$C_{LL}(x_t, x_\mu, g^2) \rightarrow \frac{x_t}{4} \left[ 1 - \frac{\alpha}{4\pi} \left( \gamma_m^{(0)} \ln \frac{m_t^2}{\mu^2} + \frac{\gamma_+}{2} \ln \frac{m_t^2}{\mu^2} - \frac{50}{3} + \frac{20}{9} \pi^2 \right) \right]. \quad (5.29)$$

In eq. (5.29) we have denoted  $\gamma^{(0)}$  by  $\gamma_+$  in order to compare it with (5.27). We make the following observations:

- (i) The last logarithm of eq. (5.27) is absent in eq. (5.29). It implies that for  $m_t \gg M_W$  the running from  $m_t$  down to low energies is in the leading approximation governed by the single operator  $\hat{O}_+ = \hat{O}_{LL}$ . Equivalently the coefficient in front of the logarithm responsible for the operator evolution is by a factor of two smaller than the one relevant for the range  $m_t \ll \mu \ll M_W$  (the last term in eq. (5.27)). A similar observation has been obtained in ref. [18].
- (ii) As can be seen from table 2, diagram (a) is responsible for the coefficient of the second logarithm in eq. (5.29). We should also stress that all other diagrams (except (f) and (g) which lead to the running of the internal quark masses) with two fictitious Higgs exchanges do not decouple and contribute to the constant term in eq. (5.29). There is however no contribution of these diagrams to the logarithmic terms. We will return to this point in subsect. 6.4, where we discuss the analysis of Datta et al. [18].
- (iii) The scales in the logarithms in eq. (5.29) indicate, that the choice  $\mu = m_t$ , instead of  $\mu = M_W$  done in subsect. 4.2, would effectively sum up all the logarithms present in the next-to-leading corrections. In this case the heavy top quark mass would be normalized at  $m_t$  and the evolution of operators would begin at  $m_t$  and not at  $M_W$  as was done until now. We will investigate this below.
- (iv) Another question which we would like to address here is whether for large  $m_t$  it would be justified to sum up the leading logarithms multiplying  $x_t$  and drop the corresponding constant terms. The answer is no! Indeed the constant pieces in question are sizeable and only for  $m_t > 6M_W$  the constant terms are less than 15% of the  $\ln x_t$  terms. For such high values of  $m_t$ , one has however to worry about perturbation in the weak coupling constant. We will elaborate on it in the summary. Thus our approach of not summing the logarithms  $\ln m_t/M_W$  is justified for all practical purposes.

## 5.6. THE CHOICE OF THE INITIAL SCALE AND OTHER DEFINITIONS OF $m_t$

We are now in a position to answer the remaining questions posed in sect. 1. Until now we have evaluated the initial conditions for the renormalization group equations at the scale  $\mu = M_W$ . This implies that also  $m_t$  is evaluated at  $M_W$ . The choice  $\mu = M_W$  is useful as in this case the  $\ln x_\mu$  terms are set to zero and eq. (3.9) simplifies. This choice is however not necessary. Let us see what happens if the

initial conditions are taken at  $\mu = aM_W$ , with  $a$  being some arbitrary constant<sup>★</sup>. We can first rewrite  $\ln x_\mu$  in (3.9) as follows

$$-\ln x_\mu = \ln \frac{a^2 M_W^2}{\mu^2} - \ln a^2. \quad (5.30)$$

Setting  $\mu = aM_W$  we are left with two new terms which are proportional to  $\ln a^2$ . These new terms will modify the next-to-leading corrections in eq. (4.17) and consequently also in eqs. (5.3), (5.15) and (5.18). In order to discuss it more explicitly let us choose  $a = m_t/M_W$ . This means that we now evolve the operator  $\hat{O}_{LL}$  from  $m_t$  down to  $\mu$  and normalize the running top quark mass at  $m_t$  ( $m_t^* \equiv \bar{m}_t(m_t)$ ). This amounts to replacing  $\alpha_s(M_W)$  by  $\alpha_s(m_t)$  and to change  $W(x_t)$  entering  $Y(x_t)$  by adding

$$\Delta W(x_t) = 6 \ln x_t \left[ \left( \frac{N-1}{2N} \right) + \left( \frac{N^2-1}{2N} \right) x_t \frac{\partial}{\partial x_t} \right] S(x_t). \quad (5.31)$$

Let us investigate the effect of these two new terms. We first note that the change in the argument of  $\alpha_s$  in the leading term cancels precisely the first term in eq. (5.31). One can verify this by expanding  $\alpha(m_t)$  around  $M_W$ . This discussion answers the second question posed in sect. 1: the result for  $\eta_2$  does not depend on the initial scale for the evolution of the operator if next-to-leading corrections have been taken into account. The case of the second term in eq. (5.31) is different. This change is related to the change in the definition of the top quark mass. There is no possibility to cancel this change by considering  $\eta_2$  alone and we therefore conclude that the QCD factors depend on the definition (normalization) of  $m_t$ . Denoting the QCD factors corresponding to  $m_t^*$  by  $\eta_2^*$ , we thus find that  $\eta_2 \neq \eta_2^*$ . This difference is however not disturbing. Indeed the physical amplitudes are calculated from  $H_{\text{eff}}$  of eq. (4.16) which involves the product  $\eta_2(x_t)S(x_t)$ . Now the value of  $S(x_t)$  depends as well on the definition of the top quark mass and this dependence cancels the one in  $\eta_2$  so that the product  $\eta_2(x_t)S(x_t)$  does not depend on this definition in the sense of eq. (5.1).

In order to illustrate this more explicitly we plot in fig. 8:

$$\bar{T}_{2B}(x_t) \equiv \bar{\eta}_{2B}(x_t)S(x_t) \quad \text{and} \quad \bar{T}_{2B}^*(x_t^*) \equiv \bar{\eta}_{2B}^*(x_t^*)S(x_t^*) \quad (5.32)$$

as functions of  $m_t$  and  $m_t^*$  respectively. We observe that  $\bar{T}_{2B}(x_t)$  and  $\bar{T}_{2B}^*(x_t^*)$  differ considerably. However also  $x_t$  and  $x_t^*$  differ (see eq. (5.33) and table 4), and consequently  $\bar{T}_{2B}(x_t) = \bar{T}_{2B}^*(x_t^*)$ , as it should. We demonstrate this in fig. 8 for  $m_t^* = 200$  GeV, for which  $m_t = 214$  GeV.

<sup>★</sup> The constant  $a$  should not be too large since such a choice would introduce large logarithms in the initial condition.

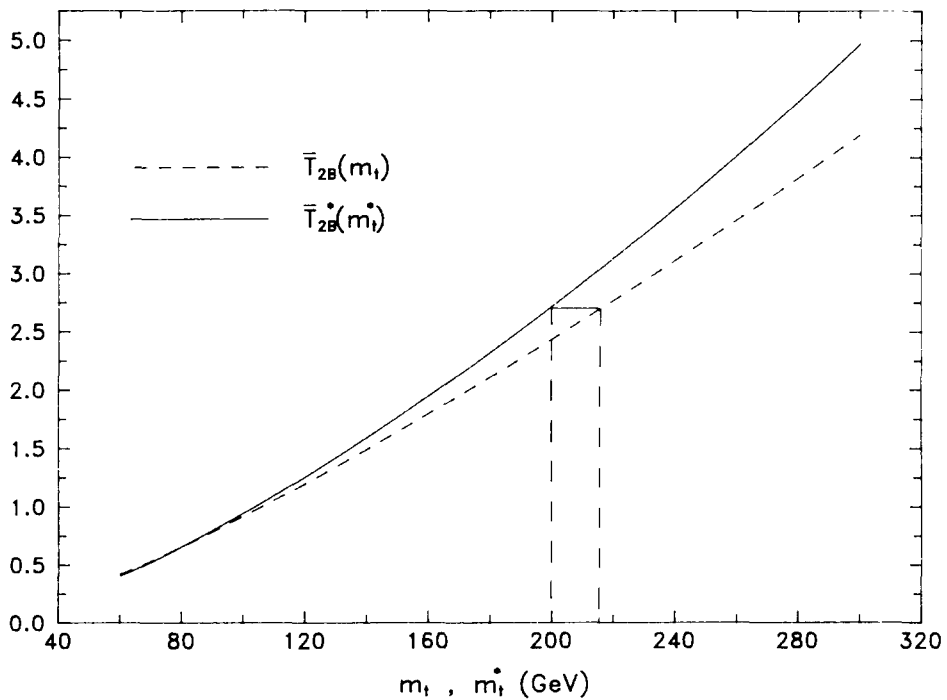


Fig. 8.  $\bar{T}_{2B}(x_1)$  and  $\bar{T}_{2B}^*(x_1^*)$  given in eq. (5.32) as functions of  $m_t$  and  $m_t^*$ . The vertical lines correspond to  $m_t^* = 200$  GeV and  $m_t = 214$  GeV.

The above discussion shows that in quoting the numerical values for  $\eta_2$  it is essential to state how the top quark mass has been defined. To our knowledge this point has not been made previously in the literature. We will present the numerical analysis for  $\eta_2^*$  in the following section.

Finally the answer to the last question in sect. 1 can be very brief because it has already been extensively elaborated in the literature. Since next-to-leading order corrections have been calculated in the  $\overline{\text{MS}}$  scheme, the coupling constant should be calculated in the same scheme, i.e.  $A_{\text{QCD}} \equiv A_{\overline{\text{MS}}}$ .

Let us end this section with the following remarks:

- (i) It is clear from our discussion that the initial scale for the evolution of operators and the normalization scale for the quark masses need not be the same. We could as well start the evolution at  $\mu = M_W$  but normalize the masses at  $\mu = aM_W$  without changing the final result.
- (ii) Our statement that  $\mu = M_W$  and  $\mu = aM_W$  give the same result for the effective hamiltonian has only perturbative character. There are of course differences for these two choices but they are of higher order in the coupling constant than the contributions included in our analysis.

TABLE 3  
The values for  $\eta_{2K}^*$ ,  $\eta_{2B}^*$  and  $\bar{\eta}_{2B}^*$  as functions of  $m_t^* \equiv \bar{m}_t(m_t)$  for different values of  $A_4$

$\eta_2^*(m_t^*)$	$m_t^* [\text{GeV}]$	$A_4 = 100 \text{ MeV}$	$A_4 = 200 \text{ MeV}$	$A_4 = 300 \text{ MeV}$
$\eta_{2K}^*(m_t^*)$	70	0.573	0.582	0.587
	90	0.571	0.580	0.585
	110	0.569	0.578	0.582
	130	0.567	0.575	0.579
	150	0.564	0.572	0.577
	200	0.559	0.566	0.570
	250	0.554	0.561	0.565
	300	0.550	0.557	0.560
$\eta_{2B}^*(m_t^*)$	70	0.539	0.553	0.561
	90	0.537	0.551	0.559
	110	0.535	0.548	0.557
	130	0.533	0.546	0.554
	150	0.531	0.543	0.551
	200	0.526	0.538	0.545
	250	0.521	0.533	0.540
	300	0.518	0.529	0.536
$\bar{\eta}_{2B}^*(m_t^*)$	70	0.892	0.878	0.867
	90	0.889	0.875	0.864
	110	0.886	0.871	0.860
	130	0.882	0.867	0.856
	150	0.878	0.863	0.852
	200	0.870	0.854	0.842
	250	0.863	0.846	0.834
	300	0.857	0.840	0.827

(iii) It follows from (ii) that the precise statement about the scales of masses and coupling constant which we can make after performing our calculation really applies only to the leading term in eqs. (4.16) and (4.17), i.e. to  $S(x_t)$  in (4.16) and to the first term in eq. (4.17). In order to be able to make similar statements about the next-to-leading terms one would have to go one step further in perturbation theory.

(iv) Similarly, whereas in the leading term of eq. (4.17) the two-loop approximation for  $\alpha(M_W)$  should be used, the one-loop approximation would suffice for the next-to-leading term.

#### 5.7. THE RESULTS FOR $\eta_{2K}^*$ , $\eta_{2B}^*$ AND $\bar{\eta}_{2B}^*$

In table 3 we show the values for  $\eta_{2K}^*$ ,  $\eta_{2B}^*$  and  $\bar{\eta}_{2B}^*$  as functions of  $m_t^* = \bar{m}_t(m_t)$ . This table should be compared with table 1, where the corresponding values for  $\eta_{2K}$ ,  $\eta_{2B}$  and  $\bar{\eta}_{2B}$  as functions of  $m_t$  have been given. A direct comparison of these two definitions for  $\eta_2$  is shown in figs. 4–6. We observe that for  $m_t \gg M_W$  the

numerical values for  $\eta_2$  and  $\eta_2^*$  differ considerably from each other. In particular the  $m_t^*$ -dependence of  $\eta_2^*$  is much weaker than the dependence of  $\eta_2$  on  $m_t$ . As was discussed in subsect. 5.6 the difference between  $\eta_2$  and  $\eta_2^*$  is attributed to the second term in eq. (5.31) and is cancelled by the change  $S(x_t) \rightarrow S(x_t^*)$ , so that eq. (5.1) is satisfied. We have checked numerically that eq. (5.1) is satisfied to better than 2% accuracy for  $m_t < 200$  GeV and to better than 5% for  $m_t < 300$  GeV, which confirms our statements made in subsect. 5.6. In testing eq. (5.1) we have used

$$\bar{m}_t(M_W) = m_t^* \left[ \frac{\alpha_5(M_W)}{\alpha_5(m_t^*)} \right]^{d_m^{(0)}} \left[ 1 + \frac{\alpha_5(M_W) - \alpha_5(m_t^*)}{4\pi} P \right], \quad (5.33)$$

$$P = \frac{\gamma_m^{(1)}}{2\beta_0} - \frac{d_m^{(0)}}{\beta_0} \beta_1, \quad d_m^{(0)} = \frac{\gamma_m^{(0)}}{2\beta_0}, \quad (5.34)$$

with  $\gamma_m^{(0)}$  and  $\gamma_m^{(1)}$  given in eq. (4.6). For completeness we also give the definition of the physical top quark mass as the pole of the renormalized propagator [25]

$$m_t^{\text{phys}}(m_t^*) = m_t^* \left[ 1 + C_F \frac{\alpha_5(m_t^*)}{\pi} \right]. \quad (5.35)$$

Various corresponding values for  $m_t^*$ ,  $\bar{m}_t(M_W)$  and  $m_t^{\text{phys}}(m_t^*)$  for  $\Lambda_{\overline{\text{MS}}} = 200$  MeV are given in table 4.

This analysis shows that much of the  $m_t$ -dependence present in  $\eta_2$  can be transferred to  $S(x_t)$  by choosing  $m_t^*$  as the top quark mass. We have anticipated this already in subsect. 5.5 by analysing eq. (5.29) in which the choice  $\mu = m_t$  would have removed the logarithmic terms. This particular feature of higher order QCD corrections, that an appropriate choice of the scale in the leading term has

TABLE 4  
The corresponding values for  $m_t^* = \bar{m}_t(m_t)$ ,  $m_t = \bar{m}_t(M_W)$  and  $m_t^{\text{phys}}(m_t^*)$  as given in eqs. (5.33) and (5.35) respectively, for  $\Lambda_4 = 200$  MeV

$m_t^* = \bar{m}_t(m_t)$ [GeV]	$m_t = \bar{m}_t(M_W)$ [GeV]	$m_t^{\text{phys}}(m_t^*)$ [GeV]
70	69.3	73.4
90	90.8	94.2
110	112.8	115.0
130	134.9	135.7
150	157.3	156.5
200	214.1	208.3
250	271.8	260.1
300	330.1	311.9



an impact on the size of the next-to-leading corrections, has been known in deep-inelastic scattering and other processes for many years. Our calculation demonstrates, that in flavour-changing neutral current processes, in which the leading term is a sensitive function of  $m_t$ , the size of the next-to-leading order corrections can be changed by changing the definition of  $m_t$ . For this reason it is important to ask how large the next-to-leading order corrections calculated by us really are.

#### 5.8. THE SIZE OF THE NEXT-TO-LEADING ORDER CORRECTIONS

We have just demonstrated that the complete result for  $\eta_2(x_t)S(x_t)$  does not depend on the definition of  $m_t$ , i.e. the scale of  $\bar{m}_t$ , nor on the scale at which the evolution to low energies has been started. Yet it is clear that, at the same time, the size of the next-to-leading order corrections depends on the choice of these scales. We illustrate this in fig. 9 by showing the ratios

$$R_K(m_t) = \frac{\eta_{2K}(x_t)}{(\eta_{2K})_{LO}}, \quad R_K^*(m_t^*) = \frac{\eta_{2K}^*(x_t^*)}{(\eta_{2K}^*(x_t^*))_{LO}}, \quad (5.36)$$

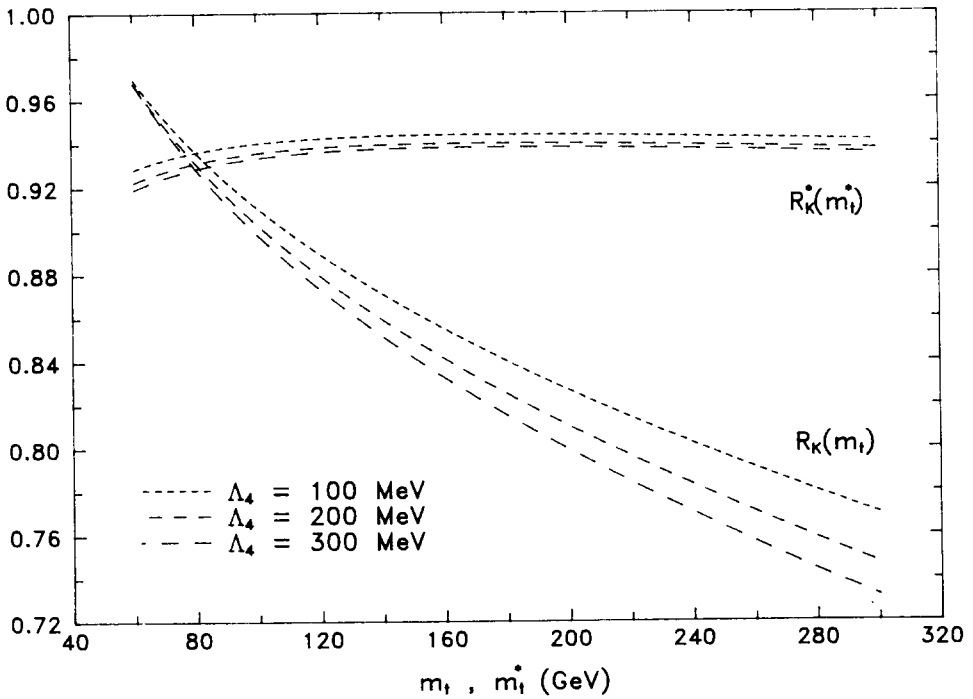


Fig. 9. The ratios  $R_K(m_t)$  and  $R_K^*(m_t^*)$  given in eq. (5.36) as functions of  $m_t$  and  $m_t^*$  for different values of  $\Lambda_4$ .

where  $(\eta_{2K}^*(x_t^*))_{\text{LO}}$  is given by eq. (1.4), with  $\alpha(M_W)$  replaced by  $\alpha(m_t^*)$ . We observe that in the first case the corrections are substantial and increase strongly with  $m_t$ . In the second case they are small and depend only weakly on  $m_t^*$ . It should also be recalled that the size of the next-to-leading term does depend on the renormalization scheme for the coupling constant, whereas this dependence is not present in the full hamiltonian. The results in fig. 9 correspond to the  $\overline{\text{MS}}$  scheme. In view of all these features it is practically impossible to state uniquely how large the next-to-leading corrections to  $H_{\text{eff}}$  are: the distribution of QCD corrections between the leading and next-to-leading terms depends on the scales given above and only the complete result is free of this dependence. This fact demonstrates the importance of next-to-leading order calculations.

### 5.9. PHENOMENOLOGICAL IMPLICATIONS FOR $B^0-\bar{B}^0$ MIXING AND $CP$ VIOLATION

As we have just seen the inclusion of next-to-leading QCD corrections removes the uncertainties related to the choices of scales present in the leading order formulae. This allows a more precise determination of the parameters of the Standard Model than was possible until now. For this reason we will calculate the element  $|V_{td}|$  as a function of  $m_t^*$  using the data on  $B^0-\bar{B}^0$  mixing.

In the Standard Model  $B^0-\bar{B}^0$  mixing is, to an excellent approximation, given by the box diagram with internal top quark propagators and consequently

$$x_d \equiv \frac{(\Delta M)_B}{\Gamma} = \tau_B \frac{G_F^2 M_W^2}{6\pi^2} m_B (B_B(m_b) F_B^2) \bar{\eta}_{2B}^*(x_t^*) S(x_t^*) |V_{td}|^2. \quad (5.37)$$

Here  $(\Delta M)_B$  is the mass difference between the mass eigenstates in the  $B_d^0-\bar{B}_d^0$  system and  $\Gamma = 1/\tau_B$ , with  $\tau_B$  being the B-meson lifetime. In our numerical analysis we will use  $\tau_B = 1.15 \times 10^{-12}$  s. The factor  $B_B(m_b)$  has been discussed in subsect. 5.2 and  $F_B$  is the B-meson decay constant resulting from the evaluation of the hadronic matrix element  $\langle \bar{B}_d^0 | (\bar{b}d)_{V-A} (\bar{b}d)_{V-A} | B_d^0 \rangle$ . There is a general belief that  $B_B(m_b) \approx 1$  and so we will set it to unity. On the other hand the value of  $F_B$  is rather uncertain, e.g.  $F_B = 175 \pm 25$  MeV as indicated by QCD sum rules [26–30].

The  $m_t$ -dependence in eq. (5.37) enters only in the product  $\bar{\eta}_{2B}^*(x_t^*) S(x_t^*)$ . Since this product is of physical relevance we provide the values for  $\bar{T}_{2B}^*(x_t^*)$ , as defined in eq. (5.32), and the analogous functions  $T_{2K}^*(x_t^*)$  and  $T_{2B}^*(x_t^*)$  for different values of  $m_t^*$  and  $\Lambda_{\text{QCD}}$  in table 5.  $T_{2K}(x_t^*)$  is of relevance for the study of the  $\varepsilon$ -parameter. Using eq. (5.37) we obtain

$$|V_{td}|(m_t^*) = 0.016 \frac{175 \text{ MeV}}{\sqrt{B_B(m_B) F_B^2}} \left[ \frac{x_d}{0.70} \frac{\bar{T}_{2B}^*(m_t^* = M_W)}{\bar{T}_{2B}^*(m_t^*)} \right]^{1/2}. \quad (5.38)$$

TABLE 5

The values for  $T_K^*$ ,  $T_B^*$  and  $\bar{T}_B^*$  as functions of  $m_t^* \equiv \bar{m}_t(m_t)$  for different values of  $A_4$ 

$T^*(m_t^*)$	$m_t^*[\text{GeV}]$	$A_4 = 100 \text{ MeV}$	$A_4 = 200 \text{ MeV}$	$A_4 = 300 \text{ MeV}$
$T_K^*(m_t^*)$	70	0.343	0.349	0.352
	90	0.521	0.528	0.533
	110	0.717	0.728	0.734
	130	0.930	0.943	0.950
	150	1.156	1.172	1.181
	200	1.779	1.802	1.814
	250	2.479	2.509	2.525
	300	3.257	3.295	3.314
$T_B^*(m_t^*)$	70	0.323	0.331	0.336
	90	0.490	0.502	0.510
	110	0.674	0.691	0.702
	130	0.874	0.895	0.909
	150	1.087	1.113	1.130
	200	1.673	1.711	1.735
	250	2.331	2.382	2.415
	300	3.063	3.128	3.170
$\bar{T}_B^*(m_t^*)$	70	0.534	0.526	0.520
	90	0.810	0.797	0.787
	110	1.116	1.097	1.083
	130	1.447	1.422	1.404
	150	1.800	1.768	1.744
	200	2.768	2.717	2.680
	250	3.858	3.784	3.730
	300	5.070	4.969	4.896

Setting  $x_d$  to its central experimental value  $x_d = 0.70$ ,  $\sqrt{B_B(m_B)F_B^2} = 175 \text{ MeV}$  and  $\bar{T}_{2B}^*(M_W) = 0.657$ , we plot in fig. 10  $|V_{td}|$  as a function of  $m_t^*$  for  $A_{\text{QCD}} = 200 \text{ MeV}$ . For comparison we show the result which one would obtain had one used the formula (5.19) for  $\bar{\eta}_{2B}$  instead of  $\bar{\eta}_{2B}^*(x_t^*)$  and  $S(x_t)$  instead of  $S(x_t^*)$ . This difference illustrates in a certain way the effect of next-to-leading order corrections.

Another application of our analysis is an improvement in the determination of the value of the phase  $\delta$  in the CKM matrix which is important for the study of  $CP$  violation. Usually this phase is obtained from the analysis of the  $CP$ -violating parameter  $\varepsilon$ . Although this analysis is again dominated by the effective hamiltonian of eq. (5.2), there are 5–10% contributions coming from the term proportional to  $\eta_3$  in eq. (1.1) for which the next-to-leading QCD corrections are unknown. In view of this we are at present not in a position to make a detailed numerical study of the impact of our calculations on the phase  $\delta$  on the basis of  $\varepsilon$ .

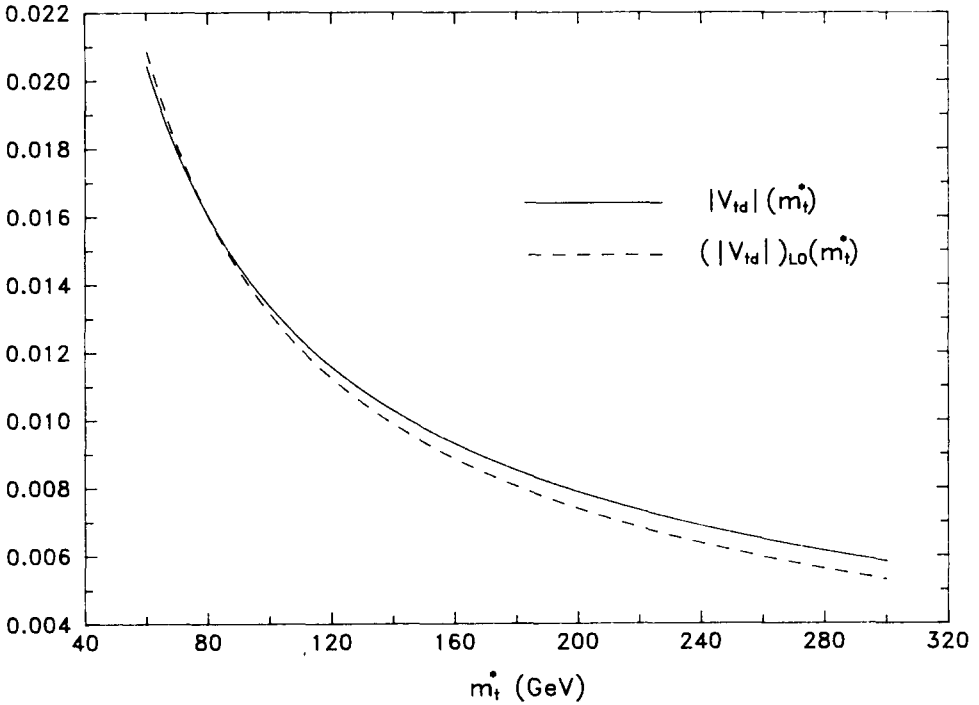


Fig. 10.  $|V_{td}|$  extracted from  $B^0-\bar{B}^0$  mixing as a function of  $m_t^*$  with (solid) and without (dashed) next-to-leading QCD corrections.

A complementary way of getting information about  $\delta$  is  $B^0-\bar{B}^0$  mixing. Indeed  $|V_{td}|$  is a sensitive function of  $\delta$ ,

$$|V_{td}| = \sqrt{a^2 + b^2 - 2ab \cos \delta} \quad \text{with} \quad a = s_{12}s_{23}, \quad b = c_{12}c_{23}s_{13}, \quad (5.39)$$

where  $s_{ij}$  and  $c_{ij}$  represent the coefficients in the standard parametrization of the CKM matrix [13,31]. In order to illustrate the effect of next-to-leading order corrections on  $\delta$ , we set the  $s_{ij}$  to their central values [32]

$$s_{12} = 0.22, \quad s_{23} = 0.046, \quad s_{13} = 0.005. \quad (5.40)$$

From  $|V_{td}|$  as given in fig. 10 and eq. (5.39), we find  $\delta$  as a function of  $m_t^*$ . The meaning of the curves shown in fig. 11 is the same as in fig. 10.

It is evident from this analysis that there is a visible impact of our new results for  $\eta_2$  on the extracted parameters of the CKM matrix. In fact our analysis is the first one which uses meaningfully the running top quark mass and the QCD scale  $\Lambda_{\overline{MS}}$  in FCNC processes. On the other hand we are well aware of the fact that the

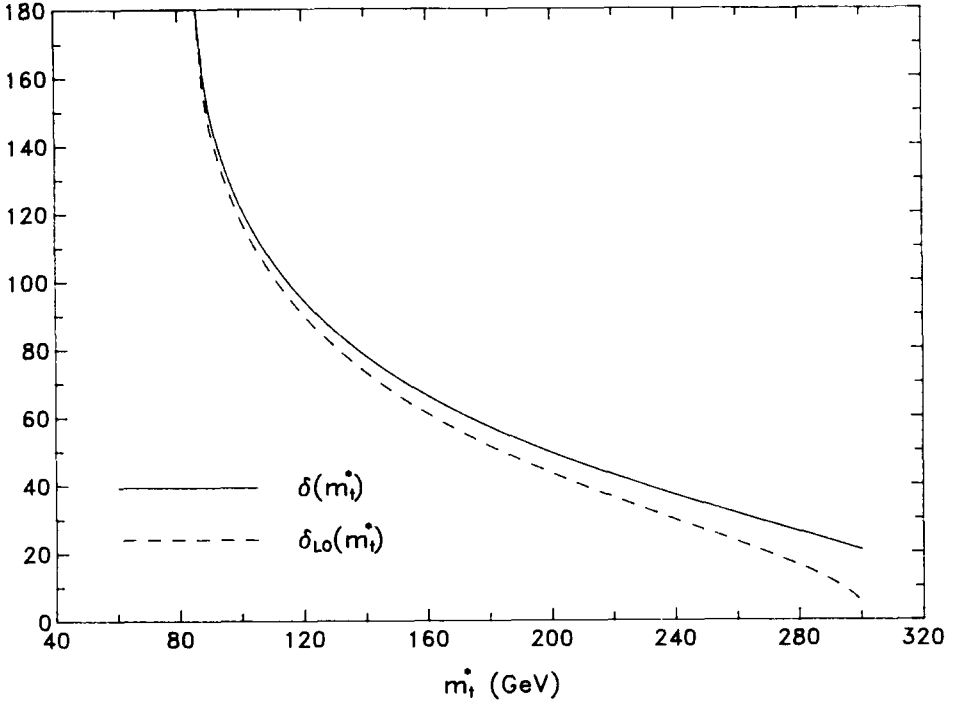


Fig. 11. The  $CP$ -violating phase  $\delta$  obtained on the basis of fig. 10 and eq. (5.39) as a function of  $m_t^*$ .

changes in  $|V_{td}|$  and  $\delta$  due to higher order QCD corrections are smaller than the uncertainties in the value of  $m_t$  and the values of the nonperturbative parameters such as  $F_B$ . Our results will consequently be more valuable once these parameters have been better estimated or experimentally measured.

## 6. Comparison with other analyses

In this section we will critically compare our analysis with corresponding studies present in the literature. We will here concentrate on refs. [15–18] which attempt to go beyond the treatment of refs. [13, 14] and consequently can be compared with our analysis of next-to-leading order corrections. In our opinion the calculations presented in these papers are incomplete. In particular the dependence of  $\eta_2$  on the definition of  $m_t$  has not been noticed at all. Furthermore none of these papers dealt with Step 2 of our approach which is essential for the proper factorization of short and long distance contributions. Let us discuss these papers one by one.

### 6.1. THE CALCULATION OF KAUFMAN AND YAO

In this paper an exact  $O(\alpha_{\text{QCD}})$  calculation of QCD corrections to the box diagram (i.e. fig. 2) has been done. In order to avoid infrared divergences the diagrams (a), (c) and (e) were evaluated with nonvanishing external quark masses whenever necessary and consequently the results of this paper can directly be compared with the ones obtained by us in sect. 2. We give here the outcome of this comparison:

(i) The authors of ref. [15] used the  $\xi = 0$  gauge and consequently could not see that the result of the evaluation of the sum of the diagrams of fig. 2 is in fact gauge dependent. It should be stressed that this gauge dependence is only present in the terms proportional to  $\tilde{S}(x_i, x_j)$ . Yet it is useful to perform the calculation in an arbitrary gauge in order to check the gauge independence of the remaining part of the result of fig. 2. This is necessary for the gauge independence of the Wilson coefficient functions obtained after Step 2 of our analysis.

(ii) Setting  $\xi = 0$  in eqs. (2.6)–(2.15) we find that our result disagrees with the one of ref. [15]. Let us first state that we agree with ref. [15] on the diagrams (a), (c), (d), (e) and (g) except for the sign of the new operators in diagrams (a) and (c). This sign is crucial for the proper factorization of short and long distance contributions. The main difference comes however in connection with the diagrams (b) and (f). Fortunately we were able to identify the origin of the disagreement in the case of diagram (b). In this diagram the authors of ref. [15] made an error in the relative sign of two terms contributing to diagram  $WH_b$ . This error leads to a remaining gauge dependence in the coefficient function of  $\hat{O}_{\text{LL}}$ . In diagram  $HH_f$  we differ in the constant term proportional to  $A(x_i, x_j)$ .

(iii) As already stated in sect. 1 we completely disagree with the treatment of the additional operators, done in ref. [15]. The main point is that Kaufman and Yao identify the coefficients of all operators resulting from the diagrams of fig. 2 with the Wilson coefficients of local operators in the operator product expansion. This is incorrect! As we have emphasized in sect. 1 and demonstrated explicitly in sect. 3 such an identification can only be made after factorization of short and long distance contributions has been done. At this stage the tensors  $\hat{T}_1$ ,  $\hat{T}_2$  and  $\hat{T}_3$  disappear from the scene and it is immaterial how large their contributions (i.e. coefficient functions and matrix elements) to the result of fig. 2 are. Since the authors of ref. [15] decided to drop these operators anyway the disagreement between our analysis and theirs is at this point only a matter of principle. Where we however really disagree is the treatment of the contributions depending on the external quarks to the operator  $\hat{O}_{\text{LL}}$ . The claim of Kaufman and Yao is that their result can be used as a guide for the scales appearing in the leading logarithmic approximation. Comparing for instance the logarithm resulting from the diagram (a) (the term  $3 \ln x_d x_b \tilde{S}(x_i, x_j)$  in eq. (2.12)) with the perturbative expansion of the Wilson coefficient function, the authors of ref. [15] conclude, that  $\mu = \sqrt{m_d m_b}$  is the appropriate choice in the  $B^0 - \bar{B}^0$  system. Yet since the result of fig. 2 cannot be compared with the Wilson coefficient function of  $\hat{O}_{\text{LL}}$ , the identification of the

appropriate scale  $\mu$  has really no basis. Moreover as we have demonstrated in sect. 3 the sensitivity to the external quark masses is not present in the Wilson coefficient function. We will return to this point below in connection with ref. [16].

## 6.2. THE ANALYSIS OF KAUFMAN, STEGER AND YAO

The authors of ref. [16] calculated  $\eta_2$  for the B-meson system in the presence of a heavy top. This is essentially only a leading order calculation<sup>\*</sup> with the choice of the scales deduced from the analysis of Kaufman and Yao [15] discussed above. The definition of  $\eta_2$ , used in ref. [16], differs from ours. One has to rescale it by  $x_t/S(x_t)$  in order to compare their  $\eta_2$  with our results. One obtains essentially the leading term of eq. (5.19), with  $m_b$  replaced by  $\sqrt{m_d m_b} \approx 210$  MeV and  $M_W$  replaced by  $m_t$ . The resulting numerical value for  $\bar{\eta}_{2B}$  ( $\bar{\eta}_{2B} \approx 0.60$ ) is substantially smaller than our  $\bar{\eta}_{2B}$ , the difference resulting to a large extent from the difference in the choice of  $\mu$ <sup>\*\*</sup>. This difference in the choice of  $\mu$  must be compensated by the fact that  $B(\mu) > B(m_b)$ . Although the result should not depend on  $\mu$ , it is questionable that it is a good idea to use  $\mu = \sqrt{m_d m_b} \approx 210$  MeV. First of all as we stressed above the guiding principle for choosing the scale of ref. [16] has really no basis. Furthermore for such a low value of  $\mu$  one cannot expect perturbation theory to work. Finally as pointed out in refs. [24, 33], the evolution of the matrix elements containing b-quarks from  $m_b$  down to  $\mu \ll m_b$  involves new types of logarithms which were not contained in the calculation of ref. [16]. For this reason we prefer to stop the evolution of the operators at  $\mu = O(m_b)$ .

## 6.3. THE ANALYSIS OF FRÉRE, KAUFMAN AND YAO

These authors performed the first analysis of next-to-leading QCD corrections to  $K^0-\bar{K}^0$  mixing. It is not straightforward to compare our analysis with theirs because Frère et al. [17] first integrate out only the W-boson, whereas we integrate out the W-boson and the top quark simultaneously. Consequently they have to deal with bilocal operators resulting from  $O(\alpha)$  corrections to the diagram of fig. 7. Such a procedure has to be used in the case of the charm contribution (the coefficient  $\eta_1$  in eq. (1.1)) but it is not necessary, as we have illustrated in subsect. 5.4, for  $m_t \approx 60$  GeV as was considered by Frère et al. We will make a more detailed comparison with ref. [17] in a subsequent paper, in which the coefficient  $\eta_1$  will be calculated. For the time being we would like to make the following comments:

(i) Our criticism concerning factorization of short and long distance contributions made in connection with ref. [15] applies also here. In particular it appears that the values of the short distance coefficients  $\eta_i$  calculated by Frère et al. depend on the values of the external quark masses. This clearly cannot be the case as we demonstrated explicitly in our paper.

<sup>\*</sup> It does not contain two-loop anomalous dimension effects and other next-to-leading corrections considered by us. Yet we thought it to be useful to comment on this paper as well.

<sup>\*\*</sup> The fact that  $\bar{\eta}_{2B}$  of ref. [16] is closer to our  $\eta_{2B}$  than to  $\bar{\eta}_{2B}$  is a pure numerical accident.

(ii) For similar reasons we do not think that the two-loop contributions of ref. [23] have been properly incorporated. The point is that the finite parts calculated by Frère et al. (the diagrams of fig. 6 of their paper) are already contained at least partially in the result of ref. [23] and consequently it seems to us that some double counting has been made.

(iii) In view of this it is not surprising that the result for  $\eta_2$  found by Frère et al. differs drastically from the one found by us. Taking into account the difference in the definition of  $\eta_2$  used in ref. [17] i.e. multiplying the result of Frère et al. by  $x_t/S(x_t)$  we find for  $m_t = 60$  GeV the value  $(\eta_{2K})_{\text{FKY}} = 0.95 \pm 0.05$  which should be compared with  $\eta_{2K} = 0.60$  from our analysis for the same value of  $m_t$ .

#### 6.4. THE ANALYSIS OF DATTA, FRÖHLICH AND PASCHOS

In a recent paper Datta et al. [18] have presented a calculation of the leading logarithmic corrections to  $\Delta S = 2$  and  $\Delta B = 2$  processes for light and heavy top quark masses. One of their main findings is that for a heavy top quark many diagrams do not contribute in the leading logarithmic approximation; in particular those diagrams where a gluon originates on an external quark line and ends up on a heavy internal top quark line. Our explicit calculation supports this claim. However we would like to stress that for a very heavy top quark the diagrams involving two fictitious Higgs exchanges dominate, and although many of them do not contribute to the leading logarithms (see subsect. 5.5) they can in principle give significant effects. In an original version of their paper [34] the authors made the statement that these diagrams decouple and so ignored them in their numerical analyses\*, although analogous diagrams involving the theoretically less relevant  $WW$ -exchange were kept. It is not possible to make a fully meaningful comparison of the results obtained in ref. [18] with ours, because these authors did not include next-to-leading order corrections, in particular the  $HH$ -diagrams discussed above, the two-loop anomalous dimension contributions and the finite terms resulting from Step 2 of our analysis. They also admit that for  $m_t$  close to  $M_W$ , their approach is less reliable and they have to interpolate their results between  $m_t \ll M_W$  and  $m_t \gg M_W$ . Equally important is that they did not specify the definition of  $m_t$  and consequently their main result, given in fig. 5 of their paper, is subject to the uncertainties related to the interpretation of what  $m_t$  really means. As we demonstrated in fig. 8, this may result in uncertainties, as large as 20%. It should also be emphasized, that in the framework of ref. [18], the question of the definition of  $m_t$  cannot even be meaningfully addressed, because the differences in the definition of  $m_t$  are of the same order in  $\alpha$  as the constant terms neglected there. It turns out however, that their results are close to ours if  $m_t$  in their paper is set to  $m_t^*$ . A closer inspection of the numerical analysis reveals that this accidental agreement is due to the partial cancellation of  $Y(x_t)$  by  $R + Z_5$  in eq.

\* It is our impression that this is also done in the published version although there, the way they arrived at their final formula is not sufficiently well described.



(5.15) and the choice of the other input parameters used in ref. [18]. We would also like to point out, that the equality of the QCD corrections for  $\Delta S = 2$ , and  $\Delta B = 2$  transitions obtained in ref. [18] is due to the omission of threshold effects in the evolution of  $\hat{O}_{LL}$  from  $M_W$  down to  $\mu$ .

In the discussion of  $B^0-\bar{B}^0$  mixing we agree with their critique of ref. [16], that  $\mu = \sqrt{m_d m_b}$  should not be selected as the low energy cutoff scale (see subsect. 6.2), but equally we see no rationale for their inclination  $\mu = \sqrt{m_s m_b}$ . Indeed we only run the coupling down to scales  $\mu = m_b$  and make numerical predictions for a given value of  $F_B$ . Here we would like to stress again, that if  $F_B$  is calculated using nonperturbative methods first at a lower scale, then relating this to the physical decay constant is a nontrivial task and involves new types of large logarithms [24, 33] which have to be summed.

## 7. Summary

In this paper we have presented a complete calculation of leading and next-to-leading QCD corrections to the QCD factors  $\eta_{2K}$  and  $\eta_{2B}$  relevant for the  $CP$ -violating  $\varepsilon$ -parameter and  $B^0-\bar{B}^0$  mixing in the presence of a heavy top quark. Our analysis consisted of three parts: (i) the evaluation of the radiative corrections to the standard box diagram, (ii) the evaluation of QCD corrections to the matrix elements of the operator  $\hat{O}_{LL}$  between quark states, and (iii) the inclusion of the two-loop anomalous dimension of  $\hat{O}_{LL}$ . Performing (i) and (ii) in an arbitrary covariant gauge we have demonstrated explicitly, that our results are gauge independent and do not depend on the infrared structure of the theory as it should be. The performance of the third part assures the independence of the results on the renormalization scheme. We have emphasized that these results only follow after a correct factorization of short and long distance contributions.

In our opinion the question of factorization has not been properly treated in the works of Kaufman et al. [15, 16] and Frère et al. [17], which also calculated QCD corrections to  $\Delta S = 2$  and  $\Delta B = 2$  transitions. In particular in refs. [15] and [17] an explicit dependence on the infrared structure of the theory is present, whereas this cannot be true for  $\eta_2$  which is supposed to include only short distance contributions. Consequently our results differ from those of these authors. On the other hand our results turn out to be close to the leading order result of Datta et al. [18] if  $m_t$  in their paper is set to  $m_t^*$ . Explicit comparisons have been given in sect. 6.

The main virtue of our analysis is the fact that after the inclusion of next-to-leading order corrections many ambiguities present in the leading order expressions are removed. In particular:

- (i) The final result for  $\eta_2$  does not depend on the scale at which the initial conditions for the evolution of the operators have been imposed.
- (ii) The presence of next-to-leading order corrections calculated in the  $\overline{MS}$  scheme allow us to use  $A_{\overline{MS}}$ , as extracted from the data on high energy processes, in the evaluation of  $\eta_2$ .

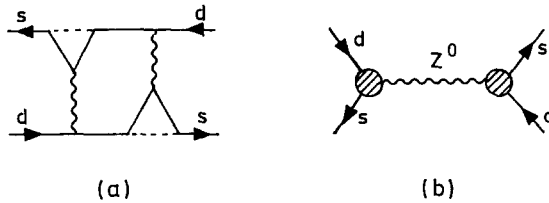


Fig. 12. (a) Typical gluonic double-penguin and (b) double- $Z^0$ -penguin diagrams contributing to  $\Delta S = 2$  transitions.

(iii) Whereas  $\eta_2$  depends on the definition of the top quark mass, the product  $T(x_t) = \eta_2(x_t)S(x_t)$  is a physical quantity.

The numerical values for  $\eta_2^*(x_t^*)S(x_t^*)$  for the K- and B-system have been collected in table 5 and can be used in phenomenological applications. We have used these results to extract  $|V_{td}|$ . The separate results for  $\eta_2$  and  $\eta_2^*$  can be found in tables 1 and 3.

In the evaluation of the QCD corrections to  $B^0-\bar{B}^0$  mixing we have set the masses of external b-quarks to zero. In our opinion the effect of  $m_b \neq 0$  can only be studied consistently in conjunction with the evaluation of hadronic matrix elements. We have also left out the gluonic double-penguin diagrams one of which is shown in fig. 12a. These are formally  $O(\alpha_{\text{QCD}}^2)$ . Moreover as analysed in great detail by Eeg and Picek [35], these diagrams although nonnegligible in the case of the coefficient  $\eta_3$ , can be safely neglected in the evaluation of  $\eta_2$  presented here.

Finally there is the question whether in the case of a very heavy top quark the contributions  $O(G_F^3)$  to  $B^0-\bar{B}^0$  mixing and  $CP$  violation could begin to play some role. The simplest, possibly the dominant contribution, arises from the double- $Z^0$ -penguin shown in fig. 12b. In the absence of QCD corrections the inclusion of this diagram in addition to the box diagram would result in the replacement

$$S(x_t) \rightarrow S(x_t) \left[ 1 + \frac{4\alpha_{\text{QED}}}{\pi \sin^2 \theta_W} \frac{C^2(x_t)}{S(x_t)} \right] = S(x_t) \left[ 1 + 0.045 \frac{C^2(x_t)}{S(x_t)} \right], \quad (7.1)$$

where  $C(x_t)$  representing the  $m_t$ -dependence of the induced  $\bar{s}dZ^0$ -vertex is given by

$$C(x_t) = \frac{x_t}{8} \left[ \frac{6 - x_t}{(1 - x_t)} + \frac{2 + 3x_t}{(1 - x_t)^2} \ln x_t \right], \quad (7.2)$$

and  $\sin^2 \theta_W \approx 0.22$ . The second term in the bracket of eq. (7.1) describes the relative size of the double- $Z^0$ -penguin and the box diagram to the Wilson coefficient function of  $\hat{O}_{LL}$ . For large values of  $m_t$  this term increases quadratically with  $m_t$ . It is however completely negligible for  $m_t \leq 150$  GeV and takes the value 0.01 for  $m_t \approx 160$  GeV. Correspondingly even for  $m_t = 300$  GeV, the highest value considered by us, the double- $Z^0$ -penguin contribution amounts to a 4% correction.

Another type of effects for such high values of  $m_t$  would be a modification of the running of  $m_t$ , due to the presence of higher order terms in the Yukawa couplings.

Probably one of the most important findings of our paper is that the short distance QCD corrections to the  $\varepsilon$ -parameter and to  $B^0-\bar{B}^0$  mixing, although sizeable for large values of  $m_t$ , have perturbative character in the framework of renormalization group improved perturbation theory. In view of the fact that the  $CP$ -violating parameter  $\varepsilon$  and  $B^0-\bar{B}^0$  mixing play important roles in the determination of the parameters of the Standard Model, these findings are very gratifying. It is to be seen whether a similar situation takes place in other flavour-changing neutral current processes.

We would like to thank K.G. Chetyrkin for interesting discussions. Particular thanks are due to Gerhard Buchalla, Michaela Harlander and Markus Lautenbacher for critically reading the manuscript.

### Note added in proof

The authors of ref. [15] have rechecked their calculation of the diagrams 2b and 2f and now agree with our results. We have also been informed by Yao about the paper by W.A. Kaufman and Y.P. Yao, Phys. Rev. D39 (1989) 3373 where the influence of the new types of logarithms found in refs. [24,33] on the  $B^0-\bar{B}^0$  system have been analyzed. In this work they recognize that the evolution of Wilson coefficient functions down to very low energy scales should involve these new logarithms, which is an improvement on the analysis of ref. [16].

### Appendix A

Here we collect the expressions for various functions which appear in the text:

$$A(x_i, x_j) = \frac{1}{(1-x_i)(1-x_j)} + \left[ \frac{x_i^2 \ln x_i}{(x_i-x_j)(1-x_i)^2} + (i \leftrightarrow j) \right], \quad (\text{A.1})$$

$$B(x_i, x_j) = \frac{1}{(1-x_i)(1-x_j)} + \left[ \frac{x_i \ln x_i}{(x_i-x_j)(1-x_i)^2} + (i \leftrightarrow j) \right]. \quad (\text{A.2})$$

The function  $I_{a,b}$  is defined by

$$I_{a,b} = \int_0^1 dt \frac{\ln t}{a-bt} = -\frac{1}{b} L_2\left(\frac{b}{a}\right), \quad (\text{A.3})$$

where  $L_2(x)$  is the dilogarithm

$$L_2(x) = -\int_0^x dt \frac{\ln(1-t)}{t} = \sum_{n=1}^{\infty} \frac{x^n}{n^2}, \quad |x| < 1. \quad (\text{A.4})$$

The function  $I_{a,b}$  satisfies the following useful relation

$$I_{i,i-j} - I_{j,j-i} = \frac{1}{2(x_i - x_j)} \ln^2 \left( \frac{x_i}{x_j} \right), \quad (\text{A.5})$$

where we use the shorthand notation  $I_{a,b} \equiv I_{x_a, x_b}$ .

In order to derive asymptotic expansions, the following relations for  $L_2(x)$  are useful:

$$L_2(x) + L_2(1-x) + \ln x \ln(1-x) = \frac{\pi^2}{6}, \quad (\text{A.6})$$

$$L_2\left(-\frac{1}{x}\right) + L_2(-x) + \frac{1}{2} \ln^2 x = -\frac{\pi^2}{6}, \quad x > 0. \quad (\text{A.7})$$

From these relations one obtains, for example, the following asymptotic expansions for the  $I$ -function:

$$I_{1,1-x} = -\frac{1}{6}\pi^2 + \left[1 - \frac{1}{6}\pi^2 - \ln x\right]x + \left[\frac{5}{4} - \frac{1}{6}\pi^2 - \frac{3}{2}\ln x\right]x^2, \quad x \ll 1, \quad (\text{A.8})$$

$$I_{1,1-x} = -\left[\frac{1}{6}\pi^2 + \frac{1}{2}\ln^2 x\right]\frac{1}{x} + \left[1 - \frac{1}{6}\pi^2 + \ln x - \frac{1}{2}\ln^2 x\right]\frac{1}{x^2}, \quad x \gg 1. \quad (\text{A.9})$$

## Appendix B

We present here the result for the diagrams of fig. 2. Decomposing the functions  $L^{(8)}(x_i, x_j)$  and  $L^{(1)}(x_i, x_j)$  introduced in eqs. (2.12) and (2.13) as follows

$$L^{(8)}(x_i, x_j) = WW^{(8)}(x_i, x_j) + 2WH^{(8)}(x_i, x_j) + HH^{(8)}(x_i, x_j) \quad (\text{B.1})$$

$$L^{(1)}(x_i, x_j) = WW^{(1)}(x_i, x_j) + 2WH^{(1)}(x_i, x_j) + HH^{(1)}(x_i, x_j), \quad (\text{B.2})$$

we obtain

$$\begin{aligned} WW^{(8)} = & \left\{ \frac{-6}{(1-x_i)(1-x_j)} + \frac{5}{2}A_{ij} - 4B_{ij} - \frac{2}{(1-x_i)(1-x_j)(x_i-x_j)} \right. \\ & \times \left[ [4 - 6(x_i + x_j - 2x_ix_j) + 3x_i^2(1-x_j)]I_{1,1-i} \right. \\ & \left. \left. + x_i^2(3 + 2x_i - 9x_j)I_{i,i-1} - 2x_i^2(x_i - 3x_j)I_{i,i-j} \right] + (i \leftrightarrow j) \right\}, \quad (\text{B.3}) \end{aligned}$$

$$\begin{aligned} WH^{(8)} = & 6x_ix_j \left\{ \frac{1}{(1-x_i)(1-x_j)} + \frac{x_i}{(1-x_i)(1-x_j)(x_i-x_j)} \right. \\ & \left. \times \left[ (2-x_j)I_{1,1-i} - x_j[I_{i,i-1} - I_{i,i-j}] \right] + (i \leftrightarrow j) \right\}, \quad (\text{B.4}) \end{aligned}$$

$$HH^{(8)} = \frac{1}{6} x_t x_{t'} x_f \left\{ \frac{(1-x_t)(1-x_{t'})}{2} - \frac{2}{7} \mathcal{A}_{t'} + 2B_{t'} + \frac{(1-x_{t'})}{2} (1-x_t) \right\} \times \left[ I_{1,1,1-t'}(2(1-3x_t) - 3x_t^2(1-x_f)) I_{1,1,1-t'} \right]$$

$$+ x_t^2(3-2x_t+3x_f) I_{t,t',1-t} + 2x_t^2(x_t-3x_f) I_{t,t',-t'} \left[ (1 \leftrightarrow f) \right],$$

(B.5)

$$\left\{ \frac{(1-x_t)(1-x_{t'})}{-3} - \frac{2}{5} \mathcal{A}_{t'} + 3B_{t'} + 2[4-3 \ln x_t] \frac{(x_t-x_{t'})}{x_t \mathcal{A}_{t'}} \right\} =$$

$$+ \frac{(1-x_{t'})(1-x_t)(x_t-x_{t'})}{9x_{t'}} \left[ 2(x_t+x_f-2x_t x_f)(1-x_f) I_{1,1,1-t'} \right]$$

$$- x_t x_{t'} [3(1-x_f)(1+x_t-2x_f)] I_{t,t',-1}$$

$$+ \frac{(1-x_t x_{t'})}{x_t x_{t'}} \left[ (1-x_t)^2 + (1-x_{t'})^2 \right] I_{t,t',-t'} \left[ (1 \leftrightarrow f) \right],$$

(B.6)

$$\left\{ \frac{(1-x_t)(1-x_{t'})}{3} - \frac{2}{11} B_{t'} - 2[4-3 \ln x_t] \frac{(x_t-x_{t'})}{x_t B_{t'}} \right\}$$

$$+ \frac{(1-x_t)(1-x_{t'})}{9} \frac{(x_t-x_{t'})}{x_t}$$

$$\times \left[ x_t x_{t'} - x_f - 2x_t x_f (1-x_f) I_{1,1,1-t'} + x_t x_f (2-x_t-x_f) I_{t,t',-1} \right]$$

$$- \frac{(1-x_{t'})}{x_{t'}} \left[ x_t x_{t'} - x_f + x_t x_f (4-x_t-x_f) I_{t,t',-t'} \right] + (1 \leftrightarrow f),$$

(B.7)

$$\left\{ -3(3-x_t-x_{t'})(1-x_f) \frac{(1-x_{t'})}{x_t x_{t'}} + \frac{2}{11} \mathcal{A}_{t'} + 3B_{t'} - \frac{(1-x_t)(1-x_{t'})}{9x_t x_{t'}} \ln x_f \right\}$$

$$+ 2[4-3 \ln x_t] \frac{(x_t-x_{t'})}{x_t \mathcal{A}_{t'}} - \frac{(1-x_t)(1-x_{t'})}{9} \frac{(x_t-x_{t'})}{x_t}$$

$$\times \left[ (1-x_t^2)(x_t-x_f) 2x_t x_{t'} I_{1,1,1-t'} \right]$$

$$+ (1-x_t)(x_t-x_f) 2x_t x_{t'} I_{t,t',-1}$$

$$- \frac{(1-x_{t'})}{x_t x_{t'}} (2-x_t-x_{t'}) I_{t,t',-t'} \left[ (1 \leftrightarrow f) \right] +$$

(B.8)

## References

- [1] M. Kobayashi and K. Maskawa, *Prog. Theor. Phys.* 49 (1973) 652
- [2] S.L. Glashow, J. Iliopoulos and L. Maiani, *Phys. Rev. D* 2 (1970) 1258
- [3] M.K. Gaillard and B.W. Lee, *Phys. Rev. D* 10 (1974) 897
- [4] A.I. Vainshtein, V.I. Zakharov and M.A. Shifman, *JETP* 45 (1977) 670
- [5] F.J. Gilman and M.B. Wise, *Phys. Rev. D* 20 (1979) 2392
- [6] V. Vysotskii, *Sov. J. Nucl. Phys.* 31 (1980) 797
- [7] B. Guberina and R.D. Peccei, *Nucl. Phys. B* 163 (1980) 289
- [8] F.J. Gilman and M.B. Wise, *Phys. Rev. D* 27 (1983) 1128
- [9] B. Grinstein, R. Springer and M.B. Wise, *Phys. Lett. B* 202 (1988) 138
- [10] C.O. Dib, I. Dunietz and F.J. Gilman, *Phys. Lett. B* 218 (1989) 487; *Phys. Rev. D* 39 (1989) 2639
- [11] J.M. Flynn and L. Randall, *Phys. Lett. B* 224 (1989) 221
- [12] J.M. Flynn and L. Randall, *Nucl. Phys. B* 326 (1989) 31
- [13] G. Buchalla, A.J. Buras and M.K. Harlander, *Nucl. Phys. B* 337 (1990) 313
- [14] J.M. Flynn, *Mod. Phys. Lett. A* 5 (1990) 877
- [15] W.A. Kaufman and Y.-P. Yao, Univ. of Michigan Report UM-TH-88-04 (1988)
- [16] W.A. Kaufman, H. Steger and Y.-P. Yao, *Mod. Phys. Lett. A* 3 (1988) 1479
- [17] J.-M. Frère, W.A. Kaufman and Y.-P. Yao, *Phys. Rev. D* 36 (1987) 809
- [18] A. Datta, J. Fröhlich and E.A. Paschos, *Z. Phys. C* 46 (1990) 63
- [19] T. Inami and C.S. Lim, *Progr. Theor. Phys.* 65 (1981) 297 [Erratum: 65 (1981) 1772]
- [20] W.A. Bardeen, A.J. Buras, D.W. Duke and T. Muta, *Phys. Rev. D* 18 (1978) 3998
- [21] E.G. Floratos, D.A. Ross and C.T. Sachrajda, *Nucl. Phys. B* 129 (1977) 66 [Erratum: B139 (1978) 545]
- [22] A.J. Buras and P.H. Weisz, *Nucl. Phys. B* 333 (1990) 66
- [23] G. Altarelli, G. Curci, G. Martinelli and R. Petrarca, *Phys. Lett. B* 99 (1981) 141; B187 (1981) 461
- [24] H.D. Politzer and M.B. Wise, *Phys. Lett. B* 206 (1988) 681
- [25] J. Gasser and H. Leutwyler, *Phys. Rep.* 87 (1982) 77
- [26] T.M. Aliev and V.L. Eletskii, *Sov. J. Nucl. Phys.* 38 (1983) 936
- [27] C.A. Dominguez and N. Paver, *Phys. Lett. B* 197 (1987) 423
- [28] S. Narison, *Phys. Lett. B* 198 (1987) 104
- [29] A. Pich, *Phys. Lett. B* 206 (1988) 322
- [30] L.J. Reinders and S. Yazaki, *Phys. Lett. B* 212 (1988) 245
- [31] Review of particle properties, *Phys. Lett. B* 204 (1988) 1
- [32] M.V. Danilov, Proc. of the XIVth Int. Symposium on Lepton and photon interactions, Stanford, August 1989
- [33] M.B. Voloshin and M.A. Shifman, *Sov. J. Nucl. Phys.* 45 (1987) 292
- [34] A. Datta, J. Fröhlich and E.A. Paschos, Dortmund Preprint, DO-TH 89/2 (1989)
- [35] J.O. Eeg and I. Picek, *Phys. Lett. B* 177 (1986) 432